Alkyne Addition and Coupling Reactions of $[W_2(\eta\text{-}C_5H_4R)_2X_4]$ (X = Cl or Br) *

Qian Feng, Malcolm L. H. Green and Philip Mountford
Inorganic Chemistry Laboratory, South Parks Road, Oxford OX1 3QR, UK

The W≡W triply bonded dimers $[W_2(\eta\text{-}C_5H_4Pr^i)_2X_4]$ (X = Cl or Br) react with alkynes C_2R_2 to afford the dimetallatetrahedrane complexes $[W_2(\eta\text{-}C_5H_4Pr^i)_2X_4(\mu\text{-}C_2R_2)]$ (X = Cl, R = Et or $SiMe_3$; X = Br, R = Me, Et or Ph†) or poorly defined polynuclear complexes $[\{W(\eta\text{-}C_5H_4Pr^i)Br_2(CR)\}_{3x}]$ (R = Me or Et) depending upon the reaction conditions. Treatment of $[W_2(\eta\text{-}C_5H_4R)_2X_4]$ (X = Cl, R = Pr^i or Me; X = Br, R = Pr^i) with an excess of but-2-yne affords the corresponding flyover bridge complexes $[W_2(\eta\text{-}C_5H_4R)_2X_4(\mu\text{-}C_4Me_4)]$; treatment of $[W_2(\eta\text{-}C_5H_4Pr^i)_2Cl_4]$ with pent-2-yne gives a mixture of the isomers $[W_2(\eta\text{-}C_5H_4Pr^i)_2Cl_4\{\mu\text{-}(2,3)\text{-}C_4Et_2Me_2\}]$ and $[W_2(\eta\text{-}C_5H_4Pr^i)_2Cl_4\{\mu\text{-}(1,4)\text{-}C_4Et_2Me_2\}]$. The planar bridging C_4Me_4 moiety in the crystallographically characterised *trans*-$[W_2(\eta\text{-}C_5H_4Me)_2Cl_4(\mu\text{-}C_4Me_4)]$† is found to be perpendicular to the W–W bond and bound to each metal atom in a tetrahapto fashion. Treatment of $[W_2(\eta\text{-}C_5H_4Pr^i)_2Cl_4(\mu\text{-}C_2Et_2)]$ or $[\{W(\eta\text{-}C_5H_4Pr^i)Br_2(CEt)\}_{3x}]$ with an excess of but-2-yne affords the mixed-alkyne flyover bridge complexes $[W_2(\eta\text{-}C_5H_4Pr^i)_2X_4\{\mu\text{-}(1,2)\text{-}C_4Et_2Me_2\}]$ (X = Cl or Br). The complexes $[W_2(\eta\text{-}C_5H_4R)_2Cl_4(\mu\text{-}C_4Me_4)]$ (R = Me or Pr^i) are readily hydrolysed in wet acetone to form the corresponding monooxo complexes $[W_2(\eta\text{-}C_5H_4R)_2Cl_2O(\mu\text{-}C_4Me_4)]$†. Complexes labelled † have been crystallographically characterised.

The reactions of alkynes C_2R_2 with unsupported metal–metal triple bonds have received considerable attention over recent years, particularly with respect to the $[M_2(\eta\text{-}C_5H_5)_2(CO)_4]$ (M = Cr, W or especially Mo)[1] and $[M_2(OR)_6(py)_x]$ (M = Mo or W; R = Pr^i, CH_2Bu^t or Bu^t; py = pyridine; x = 0 or 2) systems.[2] The range of products obtained from these studies is too extensive to catalogue here, but include the 'simple' $4\pi + 4\pi$ cycloaddition products (*dimetallatetrahedranes*) which contain a $M(\mu\text{-}C_2R_2)M$ unit, the so-called *flyover-bridge* complexes which contain a $M(\mu\text{-}C_{2n}R_{2n})M$ unit (where n is most commonly 2 but may take values of 3 or 4, *i.e.* equivalent to four coupled alkyne units), and the *alkylidyne* derivatives (containing a M≡CR unit) in which complete M≡M and C≡C bond rupture has occurred.[2] However, of the large number of metal–metal triply bonded complexes known, relatively few undergo reactions with alkynes to form products of these types.

We have recently reported the W≡W triply bonded complexes $[W_2(\eta\text{-}C_5H_4R)_2X_4]$ (X = Cl, R = Pr^i **1a** or Me **1b**; X = Br, R = Me **2**)[3] and describe herein their reactions with alkynes. Part of this work has been communicated.[4]

Results and Discussion

Alkyne Addition Reactions.—Treatment of toluene solutions of the complexes $[W_2(\eta\text{-}C_5H_4Pr^i)_2X_4]$ (X = Cl **1a** or Br **2**) with *ca.* 1 equivalent‡ of alkyne C_2R_2 (R = Me, Et, Ph or $SiMe_3$) gave a colour change from emerald green to red-brown or green-brown (for X = Cl, R = Et) and the monoalkyne adducts $[W_2(\eta\text{-}C_5H_4Pr^i)_2X_4(\mu\text{-}C_2R_2)]$ (X = Cl, R = Et **3** or $SiMe_3$ **4**; X = Br, R = Me **5**, Et **6** or Ph **7**) were isolated in 40–70% yield. The new compounds **3**–**7** were characterised by elemental analysis and ^1H and ^{13}C NMR spectroscopy; for **7** an X-ray structure determination was undertaken. Characterising data and the proposed structures for **3**–**7** and all the new compounds described are given in Table 1 and Scheme 1 respectively.

Two views of the molecular structure of $[W_2(\eta\text{-}C_5H_4Pr^i)_2\text{-}Br_4(\mu\text{-}C_2Ph_2)]$ **7** are given in Fig. 1, selected bond lengths and angles are listed in Table 2 and fractional atomic coordinates in Table 3. The compound may be described as a dimetallatetrahedrane in which the $\mu\text{-}C_2Ph_2$ moiety does not bond symmetrically to the two tungsten atoms, the differences in the W–C_{ac} (where C_{ac} refers to the ligating atoms of the alkyne ligand) bond lengths being *ca.* 0.40 Å. This difference represents a deviation of θ = *ca.* 26° from the ideal perpendicular bridge geometry (where the four M–C_{ac} bond lengths are equal to each other and hence θ = 0°).

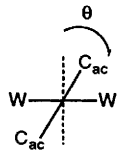

The terminal Br ligands [Br(2) and Br(4) in Fig. 1] *cis* to the $\mu\text{-}C_2Ph_2$ fragment lie either side of the imaginary plane containing the two W atoms and the centroid of the C_{ac}–C_{ac} bond and are related by a dihedral angle Br(2)–W(1)–W(2)–Br(4) of 62.9°. In contrast the Br and $\eta\text{-}C_5H_4Pr^i$ ligands *trans* to the $\mu\text{-}C_2Ph_2$ moiety are mutually eclipsed. The angles W–W–Br for the Br ligands *cis* to the alkyne ligand [*i.e.* Br(2) and Br(4)] (average 122.4°) are substantially more obtuse than those for the Br ligands [*i.e.* Br(1) and Br(3)] which lie *trans* to the alkyne ligand (average 100.5°). We presume that this reflects steric congestion imposed by the bulky bridging ligand. The movement of the *cis* Br ligands out of the W–W plane and away from the $\eta\text{-}C_5H_4Pr^i$ groups may arise from additional steric repulsion by these proximal $\eta\text{-}C_5H_4Pr^i$ ligands. The deviation of the μ-alkyne ligand in **7** from the ideal perpendicular bridging geometry may also be due to steric congestion around the metal centre.

Alternatively, Cotton[5] and others[6,7] have suggested on the basis of semi-empirical molecular orbital calculations that the deviation of a bridging alkyne from an identical perpendicular

* *Supplementary data available:* see Instructions for Authors, *J. Chem. Soc., Dalton Trans.*, 1992, Issue 1, pp. xx–xxv.

‡ Except for X = Cl, R = Et where an excess of C_2Et_2 may be used since the monoalkyne adduct **3** is insoluble in toluene and thus does not react further with any excess of C_2Et_2.

Table 1 Analytical and spectroscopic data

Compound	Colour	Analysis[a] (%) C	H	Halide	NMR data[b]
3	Olive green	32.6 (32.8)	3.85 (4.0)	17.6 (17.6)	^{1}H:[c,d] 7.52, 6.79, 6.43, 5.68 (4 × virtual q, 4 × 2 H, η-$C_5H_4Pr^i$), 5.28, 4.25 (2 × d of q, 2 × 2 H, ^2J 13.6, ^3J 7.6, CH_2Me), 2.50 (spt, 2 H, J 6.9, C*H*Me$_2$), 1.28 (t, 6 H, J 7.6, CH$_2$*Me*), 1.12, 0.95 (2 × d, 2 × 6 H, J 6.9, CH*Me*$_2$) ^{13}C-{^{1}H}:[c,d] 238.2 (μ-C_2Et_2), 140.6 (*C*Pr^i), 108.7, 107.9 (2 signals overlapping), 101.7 (4 × CH of η-$C_5H_4Pr^i$), 35.0 (*C*H$_2$Me), 27.2 (*C*HMe$_2$), 22.6, 19.3 (2 × CH*Me*$_2$), 12.6 (CH$_2$*Me*)
4	Brown	32.0 (32.2)	4.4 (4.5)	16.2 (15.9)	^{1}H: 7.89, 7.38, 5.94, 5.43 (4 × virtual q, 4 × 2 H, η-$C_5H_4Pr^i$), 2.56 (spt, 2 H, J 6.9, C*H*Me$_2$), 0.91, 0.86 (2 × d, 2 × 6 H, J 6.9, CH*Me*$_2$), 0.75 (s, 18 H, SiMe$_3$) ^{13}C: 237.3 (s, *C*SiMe$_3$), 141.5 (s, *C*Pr^i), 114.1, 111.0, 105.7, 105.5 (4 × d, J *ca.* 182, CH of η-$C_5H_4Pr^i$), 28.1 (d, J 132, *C*HMe$_2$), 23.3, 20.7 (2 × q, J 128, CH*Me*$_2$), 4.9 (q, J 120, SiMe$_3$)
5	Orange-red	25.0 (25.1)	2.9 (2.95)	33.1 (33.4)	^{1}H:[c] 7.00, 6.86, 6.15, 4.98 (4 × virtual q, 4 × 2 H, η-$C_5H_4Pr^i$), 3.68 (s, 6 H, μ-C$_2$*Me*$_2$), 3.14 (spt, 2 H, C*H*Me$_2$), 1.44, 1.29 (2 × d, 2 × 6 H, CH*Me*$_2$) ^{13}C-{^{1}H}:[c] 221.7 (μ-*C*$_2$Me$_2$), 142.4 (*C*Pr^i), 115.1, 112.7, 111.3, 105.5 (4 × CH of η-$C_5H_4Pr^i$), 27.0 (overlapping μ-C$_2$*Me*$_2$ and *C*HMe$_2$), 22.0, 21.2 (2 × CH*Me*$_2$)
6	Orange-red	26.8 (26.9)	3.3 (3.3)	32.1 (32.5)	^{1}H: 6.63, 6.51, 5.84, 4.86 (4 × virtual q, 4 × 2 H, η-$C_5H_4Pr^i$), 4.51, 4.25 (2 × d of q, 2 × 2 H, ^2J 14.9, ^3J 7.5, C*H*$_2$Me), 2.99 (spt, 2 H, C*H*Me$_2$), 1.34 (t, 6 H, J 7.5, CH$_2$*Me*), 1.21, 0.97 (2 × d, 2 × 6 H, CH*Me*$_2$) ^{13}C-{^{1}H}: 223.9 (μ-*C*$_2$Et$_2$), 144.7 (*C*Pr^i), 117.5, 113.4, 108.9, 102.5 (4 × CH of η-$C_5H_4Pr^i$), 37.3 (*C*H$_2$Me), 26.7 (*C*HMe$_2$), 22.2, 20.5 (2 × CH*Me*$_2$), 13.3 (CH$_2$*Me*)
7[e]	Orange-Red	31.8 (32.0)	2.9 (2.95)		^{1}H:[c] 7.47, 7.26 (2 × m, 4 H + 6 H, C$_6$H$_5$), 7.10, 6.98, 5.38, 5.22 (4 × virtual q, 4 × 2 H, η-$C_5H_4Pr^i$), 3.05 (spt, 2 H, C*H*Me$_2$), 1.50, 1.26 (2 × d, 2 × 6 H, CH*Me*$_2$) ^{13}C-{^{1}H}:[c] 212.1 (μ-*C*$_2$Ph$_2$), 146.3 (*ipso*-C of C$_6$H$_5$), 144.6 (*C*Pr^i), 129–127 (CH of C$_6$H$_5$), 120.6, 113.0, 107.2, 106.7 (4 × CH of η-$C_5H_4Pr^i$), 26.2 (*C*HMe$_2$), 22.6, 19.8 (2 × CH*Me*$_2$)
8	Green-brown	25.0 (25.1)	2.9 (2.95)	33.1 (33.4)	^{1}H:[c,f] 7.60, 6.66, 6.60, 5.85, 5.72, 5.64, 5.59, 5.45, 5.38, 4.94, 4.92, 4.70 (12 × virtual q, 12 × 1 H, η-$C_5H_4Pr^i$), 4.12, 3.70, 3.58 (3 × s, 3 × 3 H, CMe), 2.79 (two signals overlapping), 2.56 (3 × spt, 2 H + 1 H, C*H*Me$_2$), 1.38–1.09 (18 H, CH*Me*$_2$)
9	Green-brown	26.8 (26.9)	3.3 (3.3)	32.1 (32.5)	^{1}H:[c,f] 7.70, 6.88, 6.51, 5.84 (4 × virtual q, 4 × 1 H, η-$C_5H_4Pr^i$), 5.81 (overlapping 2 × virtual q, 2 H, η-$C_5H_4Pr^i$), 5.71, 5.57, 5.44, 5.19, 5.06, 4.76 (6 × virtual q, 6 × 1, η-$C_5H_4Pr^i$), 4.70, 4.53, 4.48, 4.00 (4 × d of q, 4 × 1 H, C*H*$_2$Me), 3.68 (spt, 1 H, C*H*Me$_2$), 3.35 (d of q, 1 H, C*H*$_2$Me), 2.77, 2.44 (2 × spt, 2 × 1 H, C*H*Me$_2$), 1.38 (t, 3 H, CH$_2$*Me*), 1.34, 1.30, 1.22, 1.14 (4 × d, 4 × 3 H, CH*Me*$_2$), 1.13 (t, 3 H, CH$_2$*Me*), 1.10 (d, 3 H, CH*Me*$_2$), 1.09 (t, 3 H, CH$_2$*Me*), 0.97 (d, 3 H, CH*Me*$_2$)[g] ^{13}C-{^{1}H}:[c,f] 238.7, 220.2, 161.5 (3 × *C*Et), 141.5, 136.7, 127.7 (3 × *C*Pr^i), 110.4, 109.5 (two signals overlapping) 109.2, 106.5, 103.5, 99.9, 98.5, 97.5, 95.7, 94.9, 88.0 (12 × CH of η-$C_5H_4Pr^i$), 41.9, 39.7, 34.0 (3 × *C*H$_2$Me), 29.3, 28.8 (two signals overlapping) (3 × *C*HMe$_2$), 22.4, 21.4, 20.2 (3 × CH*Me*$_2$), 17.8 (two signals overlapping), 14.1 (3 × CH$_2$*Me*)
10a	Purple	34.3 (34.6)	4.0 (4.1)	16.6 (17.0)	^{1}H:[h] 5.66, 5.11 (2 × virtual t, 2 × 4 H, η-$C_5H_4Pr^i$), 3.53 [s, 6 H, μ-(1)- and μ-(4)-C$_4$Me$_4$], 3.21 (spt, 2 H, C*H*Me$_2$), 1.75 [s, 6 H, μ-(2)- and μ-(3)-C$_4$Me$_4$], 1.29 (d, 12 H, CH*Me*$_2$) ^{13}C:[h] 188.3 [s, μ-(1)- and μ-(4)-*C*$_4$Me$_4$], 143.7 (s, *C*Pr^i), 102.1 (d, J 181, CH of η-$C_5H_4Pr^i$), 101.3 [s, μ-(2)- and μ-(3)-*C*$_4$Me$_4$], 99.1 (d, J 184, CH of η-$C_5H_4Pr^i$), 33.3 [q, J 128, μ-(1)- and μ-(4)-C$_4$*Me*$_4$], 22.5 (q, J 126, CH*Me*$_2$), 15.8 [q, J 131, μ-(2)- and μ-(3)-C$_4$*Me*$_4$][i]
10b	Purple	30.95 (30.7)	3.3 (3.4)	18.0 (18.3)	^{1}H:[h] 5.52, 5.32 (2 × virtual t, 2 × 4 H, η-C_5H_4Me), 3.46 [s, 6 H, μ-(1)- and μ-(4)-C$_4$Me$_4$], 2.36 (s, 6 H, η-C$_5$H$_4$*Me*), 1.75 [s, 6 H, μ-(2)- and μ-(3)-C$_4$Me$_4$]
11	Purple	28.4 (28.6)	3.4 (3.4)	31.8 (31.7)	^{1}H:[c] 5.36, 4.82 (2 × virtual t, 2 × 4 H, η-$C_5H_4Pr^i$), 3.66 [s, 6 H, μ-(1)- and μ-(4)-C$_4$Me$_4$], 3.51 [s, 6 H, μ-(2)- and μ-(3)-C$_4$Me$_4$], 2.30 (spt, 2 H, C*H*Me$_2$), 1.30 (d, 12 H, CH*Me*$_2$) ^{13}C-{^{1}H}:[c] 185.7 [J(^{13}C–^{183}W) 44 (27% by area), μ-(1)- and μ-(4)-*C*$_4$Me$_4$], 141.5 (*C*Pr^i), 100.4, 97.7 (2 × CH of η-$C_5H_4Pr^i$), 95.2 [μ-(2)- and μ-(3)-*C*$_4$Me$_4$], 37.1 [μ-(1)- and μ-(4)-C$_4$*Me*$_4$], 30.4 (*C*HMe$_2$), 22.6 (CH*Me*$_2$), 15.8 [μ-(2)- and μ-(3)-C$_4$*Me*$_4$]
12a	Orange	34.4 (34.6)	4.2 (4.1)	17.2 (17.0)	^{1}H:[h] 5.88, 5.35, 5.25, 5.12 (4 × virtual t, 4 × 2 H, η-$C_5H_4Pr^i$), 3.52 [s, 6 H, μ-(1)- and μ-(4)-C$_4$Me$_4$], 3.33, 2.87 (2 × spt, 2 × 1 H, C*H*Me$_2$), 2.15 [s, 6 H, μ-(2)- and μ-(3)-C$_4$Me$_4$], 1.32, 1.25 (2 × d, 2 × 6 H, CH*Me*$_2$) ^{13}C-{^{1}H}:[h] 185.4 [J(^{13}C–^{183}W) 49 (25% by area), μ-(1)- and μ-(4)-*C*$_4$Me$_4$], 148.3, 142.9 (2 × *C*Pr^i), 103.1, 100.0, 95.2, 94.1 (4 × CH of η-$C_5H_4Pr^i$), 90.6 [μ-(2)- and μ-(3)-*C*$_4$Me$_4$], 33.6 [μ-(1)- and μ-(4)-C$_4$*Me*$_4$], 22.5, 22.0 (2 × CH*Me*$_2$), 15.8 [μ-(2)- and μ-(3)-C$_4$*Me*$_4$][i]
12b	Orange	30.55 (30.7)	3.2 (3.4)	18.6 (18.3)	^{1}H:[h] 5.79, 5.52, 5.21, 5.03 (4 × virtual t, 4 × 2 H, η-C_5H_4Me), 3.42 [s, 6 H, μ-(1)- and μ-(4)-C$_4$Me$_4$], 2.21, 2.05 (2 × s, 2 × 3 H, η-C$_5$H$_4$*Me*), 1.85 [s, 6 H, μ-(2)- and μ-(3)-C$_4$Me$_4$]

Table 1 (*continued*)

Compound	Colour	Analysis[a] (%) C	H	Halide	NMR data[b]
13	Orange	28.5 (28.6)	3.4 (3.4)	31.5 (31.7)	^{1}H:[c] 5.60, 5.21, 4.95 (3 × virtual t, 3 × 2 H, η-$C_5H_4Pr^i$), 3.70 [s, 6 H, μ-(1)- and μ-(4)-C_4Me_4], 3.29 (overlapping 2 × spt, 2 H, C*H*Me$_2$), 2.18 [s, 6 H, μ-(2)- and μ-(3)-C_4Me_4], 1.28, 1.31 (2 × d, 2 × 6 H, CH*Me*$_2$)[j] ^{13}C-{^{1}H}:[c] 181.8 [*J*(^{13}C–^{183}W) 49 (25% by area), μ-(1)- and μ-(4)-*C*$_4$Me$_4$], 146.0, 143.2 (2 × *C*Pr^i), 101.5, 98.7, 94.5, 93.1 (4 × CH of η-*C*$_5$H$_4$Pr^i), 84.2 [μ-(2)- and μ-(3)-*C*$_4$Me$_4$], 37.6 [μ-(1)- and μ-(4)-C$_4$*Me*$_4$], 30.7, 30.4 (2 × *C*HMe$_2$), 22.6, 22.1 (2 × CH*Me*$_2$), 16.6 [μ-(2)- and μ-(3)-C$_4$*Me*$_4$]
14	Orange	36.5 (36.3)	4.5 (4.45)	16.9 (16.5)	^{1}H:[c] 5.96, 5.81, 5.31, 5.24, 5.14, 5.11, 5.09, 5.01 (8 × virtual q, 8 × 1 H, η-$C_5H_4Pr^i$), 4.79 [d of q, 1 H, ^{2}*J* 15.4, ^{3}*J* 7.2, μ-(1)-C$_4$(C*H*$_2$Me)$_2$Me$_2$], 3.45 [s, 3 H, μ-(4)-C$_4$Et$_2$*Me*$_2$], 3.37 [d of q, 1 H, ^{2}*J* 15.4, ^{3}*J* 7.2, μ-(1)-C$_4$(C*H*$_2$Me)$_2$Me$_2$], 3.09, 2.92 (2 × spt, 2 × 1 H, C*H*Me$_2$), 2.61 [q, 2 H, *J* 7.7, μ-(2)-C$_4$(C*H*$_2$Me)$_2$Me$_2$], 2.16 [s, 3 H, μ-(3)-C$_4$Et$_2$*Me*$_2$], 1.34 [t, 3 H, *J* 7.2, μ-(1)-C$_4$(CH$_2$*Me*)$_2$Me$_2$], 1.32 [t, 3 H, *J* 7.7, μ-(2)-C$_4$(CH$_2$*Me*)$_2$Me$_2$], 1.30, 1.27, 1.21, 1.17 (4 × d, 4 × 3 H, CH*Me*$_2$) ^{13}C:[c] 193.7, 185.5 [2 × s, μ-(1)- and μ-(4)-*C*$_4$Et$_2$Me$_2$], 146.9, 144.2 (2 × s, *C*Pr^i), 105.6, 103.5, 101.6, 97.5, 95.9 (5 × d, *J ca.* 180, CH of η-*C*$_5$H$_4$Pr^i), 93.9 [s, μ-(2)- or μ-(3)-*C*$_4$Et$_2$Me$_2$], 92.8, 91.3, (2 × d, *J ca.* 180, CH of η-*C*$_5$H$_4$Pr^i), 89.8 [s, μ-(3)- or μ-(2)-*C*$_4$Et$_2$Me$_2$], 89.4 (d, *J* 179, CH of η-*C*$_5$H$_4$Pr^i), 39.6 [t, *J* 130, μ-(1)-C$_4$(*C*H$_2$Me)$_2$Me$_2$], 33.3 [q, *J* 128, μ-(4)-C$_4$Et$_2$*Me*$_2$], 29.4, 29.1 (2 × d, *J ca.* 130, *C*HMe$_2$), 25.8 [t, *J* 129, μ-(2)-C$_4$(*C*H$_2$Me)$_2$Me$_2$], 22.2, 21.7 (2 × q, *J ca.* 127, CH*Me*$_2$), 21.2 (2 × overlapping q, *J ca.* 128, CH*Me*$_2$), 16.9 [q, *J* 131, μ-(3)-C$_4$Et$_2$*Me*$_2$], 14.8, 10.0 [2 × q, *J ca.* 130, μ-(1)- and μ-(2)-C$_4$(CH$_2$*Me*)$_2$Me$_2$]
15	Purple	36.4 (36.3)	4.4 (4.45)	16.05 (16.5)	^{1}H:[c] 5.92, 4.40 (2 × virtual t, 2 × 4 H, η-C$_5$*H*$_4$Pr^i), 4.36 [q, 4 H, *J* 7.5, μ-(1)- and μ-(4)-C$_4$(C*H*$_2$Me)$_2$Me$_2$], 3.27 (spt, 2 H, *J* 7.0, C*H*Me$_2$), 1.80 [s, 6 H, μ-(2)- and μ-(3)-C$_4$Et$_2$*Me*$_2$], 1.33 (d, 12 H, *J* 7.0, CH*Me*$_2$), 1.09 [t, 6 H, *J*, 7.5, μ-(1)- and μ-(4)-C$_4$(CH$_2$*Me*)$_2$Me$_2$]
16	Orange	36.2 (36.3)	4.4 (4.45)	16.3 (16.5)	^{1}H:[c] 6.59, 5.18, 5.07 (3 × virtual t, 3 × 2 H, η-C$_5$*H*$_4$Pr^i), 4.78 [d of q, 2 H, ^{2}*J* 16.1, ^{3}*J* 7.3, μ-(1)- and μ-(4)-C$_4$(C*H*$_2$Me)$_2$Me$_2$], 4.76 (virtual t, 2 H, η-C$_5$*H*$_4$Pr^i), 3.37 (spt, 1 H, *J* 6.9, C*H*Me$_2$), 3.14 [d, of q, 2 H, ^{2}*J* 16.1, ^{3}*J* 7.3, μ-(1)- and μ-(4)-C$_4$(C*H*$_2$Me)$_2$Me$_2$], 2.91 (spt, 1 H, *J* 6.9, C*H*Me$_2$), 2.11 [s, 6 H, μ-(2)- and μ-(3)-C$_4$Et$_2$*Me*$_2$], 1.33 (d, 6 H, *J* 6.9, CH*Me*$_2$), 1.28 [t, 6 H, *J* 7.3, μ-(1)- and μ-(4)-C$_4$(CH$_2$*Me*)$_2$Me$_2$], 1.18 (d, 6 H, *J* 6.9, CH*Me*$_2$)
17[k]	Orange				^{1}H:[c] 6.02, 5.70, 5.29, 5.22 (4 × virtual q, 4 × 1 H, η-C$_5$*H*$_4$Pr^i), *ca.* 5.18 (obscured η-C$_5$*H*$_4$Pr^i), 5.09 (virtual q, 1 H, η-C$_5$*H*$_4$Pr^i), *ca.* 4.8–4.7 (obscured 2 × η-C$_5$*H*$_4$Pr^i), 4.68 [d of q, 1 H, ^{2}*J* 15.8, ^{3}*J* 6.9, μ-(2)-C$_4$(C*H*$_2$Me)$_2$Me$_2$], 3.63 [s, 3 H, μ-(4)-C$_4$Et$_2$*Me*$_2$], 3.22 [d of q, 1 H, ^{2}*J* 15.8, ^{3}*J* 6.9, μ-(1)-C$_4$(C*H*$_2$Me)$_2$Me$_2$], 3.12, 2.93 (2 × spt, 2 × 1 H, *J* 7.0, C*H*Me$_2$), 2.65, 2.25 [2 × d of q, 2 × 1 H, ^{2}*J* 16.0, ^{3}*J* 6.9, μ-(3)-C$_4$(C*H*$_2$Me)$_2$Me$_2$], 1.33 [t, 3 H, *J* 6.9, μ-(1)-C$_4$(CH$_2$*Me*)$_2$Me$_2$], *ca.* 1.3–1.2 [obscured 2 × CH*Me*$_2$ and μ-(3)-C$_4$(CH$_2$*Me*)$_2$Me$_2$], *ca.* 1.17 (overlapping 2 × d, 6 H, *J* 7.0, 2 × CH*Me*$_2$)
18	Purple	30.0 (30.1)	3.6 (3.7)	30.5 (30.8)	^{1}H:[c] 5.96, 5.81, 5.31, 5.24, 5.14, 5.11, 5.09, 5.01 (8 × virtual q, 8 × 1 H, η-C$_5$*H*$_4$Pr^i), 4.79 [d of q, 1 H, ^{2}*J* 15.4, ^{3}*J* 7.2, μ-(1)-C$_4$(C*H*$_2$Me)$_2$Me$_2$], 3.45 [s, 3 H, μ-(4)-C$_4$Et$_2$*Me*$_2$], 3.37 [d of q, 1 H, ^{2}*J* 15.4, ^{3}*J* 7.2, μ-(1)-C$_4$(C*H*$_2$Me)$_2$Me$_2$], 3.09, 2.92 (2 × spt, 2 × 1 H, C*H*Me$_2$), 2.61 [q, 2 H, *J* 7.7, μ-(2)-C$_4$(C*H*$_2$Me)$_2$Me$_2$], 2.16 [s, 3 H, μ-(3)-C$_4$Et$_2$*Me*$_2$], 1.34 [t, 3 H, *J* 7.2, μ-(1)-C$_4$(CH$_2$*Me*)$_2$Me$_2$], 1.32 [t, 3 H, *J* 7.7, μ-(2)-C$_4$(CH$_2$*Me*)$_2$Me$_2$], 1.30, 1.27, 1.21, 1.17 (4 × d, 4 × 3 H, CH*Me*$_2$) ^{13}C-{^{1}H}:[c] 195.3, 184.8 [μ-(1)- and μ-(4)-*C*$_4$Et$_2$Me$_2$], 142.1 (*C*Pr^i), 103.6, 102.2, 99.9, 95.7, 95.4, 95.3 (4 × CH of η-*C*$_5$H$_4$Pr^i and μ-(2)- and μ-(3)-*C*$_4$Et$_2$Me$_2$], 42.8, 37.1 [μ-(1)-C$_4$(*C*H$_2$Me)$_2$Me$_2$ and μ-(4)-C$_4$Et$_2$*Me*$_2$], 30.4 (*C*HMe$_2$), 27.7 [μ-(2)-C$_4$(*C*H$_2$Me)$_2$Me$_2$], 22.2, 21.7 (2 × CH*Me*$_2$), 18.5 [μ-(3)-C$_4$Et$_2$*Me*$_2$], 14.8, 10.0 [μ-(1)- and μ-(2)-C$_4$(CH$_2$*Me*)$_2$Me$_2$]
19	Orange	30.0 (30.1)	3.6 (3.7)	30.6 (30.8)	^{1}H:[c] 6.07, 5.93, 5.46 (3 × virtual q, 3 × 1 H, η-C$_5$*H*$_4$Pr^i), 5.29 (overlapping 2 × virtual q, 2 H, η-C$_5$*H*$_4$Pr^i), 5.22 [d of q, 1 H, ^{2}*J* 15.0, ^{3}*J* 7.5, μ-(1)-C$_4$(C*H*$_2$Me)$_2$Me$_2$], 5.16 (overlapping 2 × virtual q, 2 H, η-C$_5$*H*$_4$Pr^i), 4.99 (virtual q, 1 H, η-C$_5$*H*$_4$Pr^i), 3.68 [s, 3 H, μ-(4)-C$_4$Et$_2$*Me*$_2$], 3.51 [d of q, 1 H, ^{2}*J* 15.0, ^{3}*J* 7.5, μ-(1)-C$_4$(C*H*$_2$Me)$_2$Me$_2$], 3.40, 3.23 (2 × spt, 2 × 1 H, C*H*Me$_2$), 2.73 [q, 2 H, *J* 7.6, μ-(2)-C$_4$(C*H*$_2$Me)$_2$Me$_2$], 2.34 [s, 3 H, μ-(3)-C$_4$Et$_2$*Me*$_2$], 1.36–1.18 [overlapping 2 × t and 4 × d, μ-(1)- and μ-(2)-C$_4$(CH$_2$*Me*)$_2$Me$_2$ and 4 × CH*Me*$_2$] ^{13}C-{^{1}H}:[c] 192.2, 183.9 [μ-(1)- and μ-(4)-*C*$_4$Et$_2$Me$_2$], 145.3, 144.3 (2 × *C*Pr^i), 106.7, 103.6, 102.2, 97.3, 95.6, 92.6, 92.0, 89.6, 88.9, 84.8 [8 × CH of η-*C*$_5$H$_4$Pr^i and μ-(2)- and μ-(3)-*C*$_4$Et$_2$Me$_2$], 43.0, 38.3 [μ-(1)-C$_4$(*C*H$_2$Me)$_2$Me$_2$ and μ-(4)-C$_4$Et$_2$*Me*$_2$], 30.7, 30.2 (2 × *C*HMe$_2$), 27.1 [μ-(2)-C$_4$(*C*H$_2$Me)$_2$Me$_2$], 22.9, 22.6, 22.1, 21.9 (4 × CH*Me*$_2$), 17.9 [μ-(3)-C$_4$Et$_2$*Me*$_2$], 16.3, 11.6 [μ-(1)- and μ-(2)-C$_4$(CH$_2$*Me*)$_2$Me$_2$]
20a	Cherry-red	36.9 (37.1)	4.4 (4.4)	9.0 (9.1)	^{1}H: 5.67, 5.25, 5.08, 4.59 (4 × virtual t, 4 × 2 H, η-C$_5$*H*$_4$Pr^i), 3.48 [s, 6 H, μ-(1)- and μ-(4)-C$_4$Me$_4$], 3.48 (spt, 1 H, C*H*Me$_2$), 3.27 [s, 6 H, μ-(2)- and μ-(3)-C$_4$Me$_4$], 2.75 (spt, 1 H, C*H*Me$_2$), 1.18, 1.12 (2 × d, 2 × 6 H, CH*Me*$_2$) ^{13}C:[h] 158.1 [s, *J*(^{13}C–^{183}W) 114 (14% by area), μ-(1)- and μ-(4)-*C*$_4$Me$_4$], 131.9, 127.3 (2 × s, *C*Pr^i), 101.4 [s, μ-(2)- and μ-(3)-*C*$_4$Me$_4$], 103.1, 100.0, 95.2, 94.1 (4 × d, *J ca.* 180, CH of η-*C*$_5$H$_4$Pr^i), 34.7 [q, *J* 129, μ-(1)- and μ-(4)-C$_4$*Me*$_4$], 28.0, 27.5 (2 × d, *J ca.* 132, CH*Me*$_2$), 22.9, 22.7 (2 × q, *J* 129, CH*Me*$_2$), 13.8 (q, *J* 128, μ-(2)- and μ-(3)-C$_4$*Me*$_4$]

Table 1 (*continued*)

Compound	Colour	Analysis[a] (%) C	H	Halide	NMR data[b]
20b	Cherry-red	33.0 (33.3)	3.5 (3.6)	9.9 (9.8)	^{1}H: 6.15, 5.18, 5.06, 4.97 (4 × virtual t, 4 × 2 H, η-C_5H_4Me), 3.24 [s, 6 H, μ-(1)- and μ-(4)-C_4Me_4], 2.29, 2.16 (2 × s, 2 × 3 H, η-C_5H_4*Me*), 1.64 [s, 6 H, μ-(2)- and μ-(3)-C_4Me_4]

[a] Calculated values given in parentheses; halide = Cl or Br as appropriate. [b] At 25 °C in [$^2H_6$]benzene unless stated otherwise. Data given as: chemical shift (δ), multiplicity (s = singlet, d = doublet, t = triplet, q = quartet, spt = septet, m = multiplet), relative intensity, coupling constant (in Hz) and assignment; for virtually coupled multiplets the apparent coupling constant is not given; for ^{1}H NMR spectra *J* refers to the ^{1}H–^{1}H coupling constant, for ^{13}C NMR to the ^{13}C–^{1}H coupling constant unless stated otherwise. [c] In [$^2H_2$]dichloromethane. [d] At −30 °C. [e] Analysis for **7**·CH_2Cl_2. [f] At −40 °C. [g] A further d of q CH_2Me resonance is partially obscured by the residual protio-solvent resonance. [h] In [$^2H_6$]acetone. [i] The *C*HMe$_2$ resonance is obscured by the residual solvent *C*D$_3$ resonance. [j] A further η-C_5H_4Pr^i ligand proton is obscured by the residual protio-solvent resonance. [k] This compound was characterised as the major component of a *ca.* 2:1 mixture of **17** and **16** by ^{1}H NMR spectroscopy only.

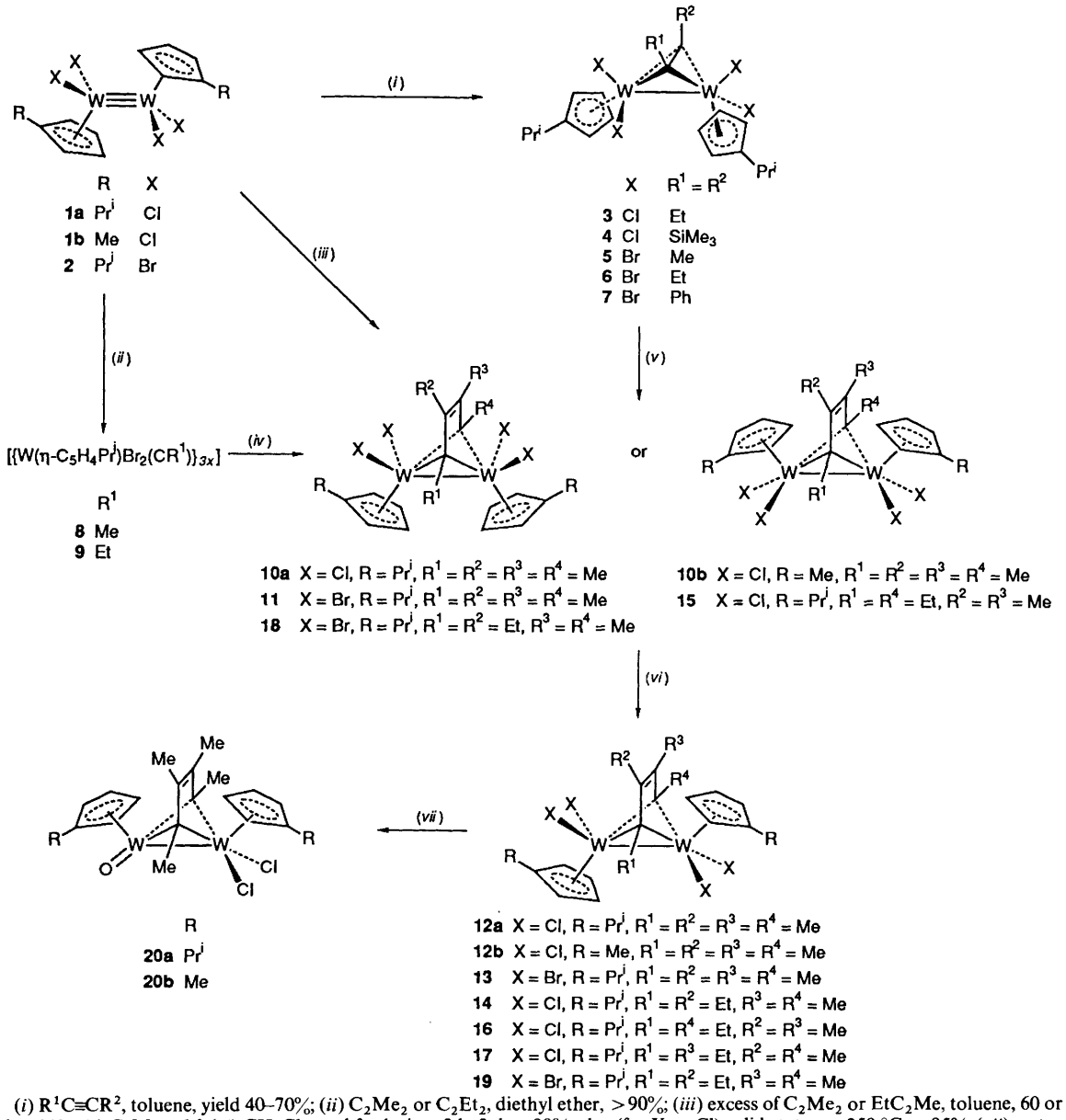

Scheme 1 (*i*) R^{1}C≡CR^2, toluene, yield 40–70%; (*ii*) C_2Me_2 or C_2Et_2, diethyl ether, >90%; (*iii*) excess of C_2Me_2 or EtC_2Me, toluene, 60 or 20%; (*iv*) C_2Me_2, thf, >80%; (*v*) C_2Me_2, thf; (*vi*) CH_2Cl_2 or thf solution, 2 h–2 d, >90%; also (for X = Cl) solid state, *ca.* 250 °C, >95%; (*vii*) water–acetone, >80%

geometry may be due to a small gap between the highest occupied (HOMO) and lowest unoccupied (LUMO) molecular orbitals (in the idealised perpendicular geometry) from which a second-order Jahn–Teller effect arises. We cannot discount such an explanation of the geometry found for the W_2(μ-C_2Ph_2) unit in **7**.

The W–W and C_{ac}–C_{ac} bond lengths in compound **7** are suggestive of substantial back donation of π-electron density from the W_2 centre to the π* orbitals of the μ-alkyne ligand. The metal–metal bond length [W(1)–W(2) 2.795(3) Å] is somewhat shorter than that found in the related carbonyl-supported complexes [M_2(η-C_5H_5)$_2$(CO)$_4$(μ-C_2H_2)] (M = Mo or W, M–M ≈ 2.98 Å)[8] and longer than those in the alkoxide-supported complexes [W_2(OR)$_6$(μ-C_2H_2)(py)$_x$] (R = Pr^i,

CH_2Bu^t or Bu^t; x = 1 or 2; W–W ≈ 2.57–2.67 Å) of Chisholm *et al.*[9] The C_{ac}–C_{ac} bond length in **7** [C(1)–C(2) 1.41(4) Å] is subsantially longer than that found for the free alkyne (C_{ac}–C_{ac} *ca.* 1.20 Å) and apparently closer to those of the co-ordinated alkyne in the alkoxide-supported (C_{ac}–C_{ac} *ca.* 1.40 Å) than in the carbonyl-supported complexes (C_{ac}–C_{ac} *ca.* 1.34 Å). However, the relatively large experimental errors associated with the C_{ac}–C_{ac} values available compared to the differences between successive values from one complex to the next make comparisons of these data less reliable.

The NMR spectroscopic data for compound **7** indicate that the molecular structure found in the solid state is maintained in solution. Furthermore, the spectroscopic data for **3**–**6** (Table 1) suggest that these complexes have similar structures to that of **7**. The ^{13}C NMR resonances of the C_{ac} atoms for the complexes **3**–**7** are found in the range δ 212–237. These values are substantially downfield of those reported for carbonyl-(δ *ca.* 70) or alkoxide-supported μ-alkyne complexes (δ 120–166). They are, however, similar to those for other predominantly halide-supported complexes such as $[W_2Cl_4(\mu\text{-}NMe_2)_2(\mu\text{-}C_2Me_2)(py)_2]$ [δ(C_{ac}) 214][10] or $[W_2Cl_4(\mu\text{-}Cl)_2(\mu\text{-}C_2R_2)(thf)_2]$ (R = H, Me or Et; thf = tetrahydrofuran) [δ(C_{ac}) 230–235].[11]

It was not possible to isolate an intermediate monoalkyne adduct $[W_2(\eta\text{-}C_5H_4Pr^i)_2Cl_4(\mu\text{-}C_2Me_2)]$ from the reaction of complex **1a** with C_2Me_2 (although the bromide-supported analogue **5** has been obtained). Addition of a single equivalent of C_2Me_2 to a toluene solution of **1a** afforded only coupled alkyne product (see below) and unreacted **1a**.

In contrast to the reactions of $[W_2(\eta\text{-}C_5H_4Pr^i)_2Br_4]$ **2** with C_2Me_2 or C_2Et_2 in toluene solution it was found that treatment of a suspension of **2** in diethyl ether with an excess of C_2Me_2 (at −20 °C) or C_2Et_2 (at room temperature) gave grey-green solids which analysed for $[\{W(\eta\text{-}C_5H_4Pr^i)Br_2(CR)\}_x]$ (R = Me **8** or Et **9**) and were further characterised by ^1H (**8**) or ^1H and $^{13}C\text{-}\{^1H\}$ (**9**) NMR spectroscopy. The ^1H NMR spectra of complexes **8** and **9** showed that they are fluxional at room temperature but static (on the NMR time-scale) at 230 K when the spectra revealed *three* types of R group (intensities 1:1:1) and three diastereotopic $\eta\text{-}C_5H_4Pr^i$ ring environments (intensities 1:1:1). Furthermore, the $^{13}C\text{-}\{^1H\}$ NMR spectrum of **9** showed, in addition to resonances characteristic of three types of R and $\eta\text{-}C_5H_4Pr^i$ ligands, three further resonances assignable to C_{ac} atoms at δ 238.7, 220.2 and 161.6. There was no evidence for a ν(C≡C) absorption in the IR spectra of either **8** or **9**. Unfortunately it was not possible further to characterise these materials. Repeated attempts to grow single crystals suitable for an X-ray diffraction analysis proved unsuccessful, and attempts to determine the molecular weight by mass spectral or solution techniques failed to give reproducible results. The ratios of the $\eta\text{-}C_5H_4Pr^i$ and R group resonances do not change with successive recrystallisations and we can thus far only characterise **8** and **9** as having the general formula $[\{W(\eta\text{-}C_5H_4Pr^i)Br_2(CR)\}_{3x}]$ where x represents an integer.

Alkyne Coupling Reactions.—When a toluene solution of $[W_2(\eta\text{-}C_5H_4Pr^i)_2Cl_4]$ **1a** was treated with an excess of C_2Me_2 at room temperature over 12 h a purple microcrystalline compound **10a** which analysed as $[W_2(\eta\text{-}C_5H_4Pr^i)_2Cl_4(C_2Me_2)_2]$ was obtained in 60% yield. The ^1H NMR spectrum showed signals assignable to a $\eta\text{-}C_5H_4Pr^i$ ring and two further resonances at δ 3.53 and 1.75 both of which integrate as 3 H relative to each Pr^i group. The ^{13}C NMR spectrum showed, in addition to signals characteristic of a $\eta\text{-}C_5H_4Pr^i$ ligand, two quartets at δ 33.3 and 15.8 and two singlets at δ 188.3 and 101.3 assignable to quaternary carbon atoms.

Similarly, treatment of complex **1b** or **2** with an excess of C_2Me_2 in toluene or diethyl ether at room temperature afforded purple compounds **10b** or **11** which analysed as $[W_2(\eta\text{-}C_5H_4R)_2X_4(C_2Me_2)_2]$ (R = Me, X = Cl; R = Pr^i, X = Br,

Table 2 Selected bond lengths (Å) and angles (°) with estimated standard deviations (e.s.d.s) in parentheses and dihedral angles (°) for $[W_2(\eta\text{-}C_5H_4Pr^i)_2Br_4(\mu\text{-}C_2Ph_2)]$ **7**; $Cp_{cent(1)}$ and $Cp_{cent(2)}$ refer to the computed $\eta\text{-}C_5H_4Pr^i$ ring centroids for W(1) and W(2) respectively

W(1)–W(2)	2.795(3)	W(1)–C(1)	1.988(9)
W(1)–Br(1)	2.589(5)	W(1)–C(2)	2.38(1)
W(1)–Br(2)	2.649(6)	W(2)–C(1)	2.39(1)
W(2)–Br(3)	2.594(5)	W(2)–C(2)	1.979(9)
W(2)–Br(4)	2.638(5)	C(1)–C(2)	1.41(4)
W(1)–$Cp_{cent(1)}$	2.02	W(2)–$Cp_{cent(2)}$	2.03
W(2)–W(1)–Br(1)	100.2(1)	W(1)–W(2)–Br(3)	100.7(1)
W(2)–W(1)–Br(2)	124.2(1)	W(1)–W(2)–Br(4)	120.6(1)
C(2)–C(1)–C(11)	132.5(15)	C(1)–C(2)–C(21)	130.2(15)
W(2)–W(1)–$Cp_{cent(1)}$	126.4	W(1)–W(2)–$Cp_{cent(2)}$	130.2

Br(2)–W(1)–W(2)–Br(4)	62.9
C(11)–C(1)–C(2)–C(21)	37.8
Br(1)–W(1)–W(2)–Br(3)	131.4
Br(1)–W(1)–W(2)–$Cp_{cent(2)}$	0.7
Br(3)–W(2)–W(1)–$Cp_{cent(1)}$	2.7

Table 3 Fractional atomic coordinates for the non-hydrogen atoms of $[W_2(\eta\text{-}C_5H_4Pr^i)_2Br_4(\mu\text{-}C_2Ph_2)]\cdot 0.5CH_2Cl_2$ **7**·$0.5CH_2Cl_2$

Atom	x	y	z	Atom	x	y	z
W(1)	0.1903(2)	0.0757(2)	0.3418(2)	C(101)	−0.073(5)	−0.056(2)	0.242(3)
W(2)	0.3679(2)	0.0293(2)	0.2044(2)	C(102)	−0.065(4)	−0.016(3)	0.348(3)
Br(1)	0.2743(6)	−0.0053(5)	0.4572(4)	C(103)	−0.025(4)	0.097(3)	0.392(2)
Br(2)	0.2850(6)	0.2482(4)	0.5243(4)	C(104)	−0.003(4)	0.132(2)	0.318(3)
Br(3)	0.1674(6)	−0.0577(4)	0.0316(4)	C(105)	−0.031(5)	0.038(3)	0.225(2)
Br(4)	0.4726(6)	0.1635(4)	0.1276(4)	C(106)	−0.095(4)	−0.171(2)	0.166(3)
C(1)	0.302(3)	0.184(1)	0.299(2)	C(107)	−0.246(5)	−0.206(4)	0.091(4)
C(2)	0.434(2)	0.167(1)	0.333(1)	C(108)	−0.103(6)	−0.244(4)	0.219(4)
C(11)	0.284(4)	0.277(2)	0.282(3)	C(201)	0.438(3)	−0.126(2)	0.203(2)
C(12)	0.185(4)	0.254(2)	0.192(3)	C(202)	0.538(3)	−0.024(2)	0.284(2)
C(13)	0.155(4)	0.338(3)	0.180(2)	C(203)	0.613(3)	0.040(2)	0.242(2)
C(14)	0.223(4)	0.445(2)	0.257(3)	C(204)	0.563(3)	−0.016(2)	0.136(2)
C(15)	0.321(4)	0.468(2)	0.346(2)	C(205)	0.453(3)	−0.119(2)	0.111(2)
C(16)	0.352(4)	0.384(3)	0.359(2)	C(206)	0.332(3)	−0.217(2)	0.217(3)
C(21)	0.581(2)	0.244(2)	0.411(2)	C(207)	0.225(5)	−0.300(4)	0.112(3)
C(22)	0.698(3)	0.320(2)	0.389(2)	C(208)	0.435(5)	−0.266(4)	0.254(4)
C(23)	0.826(3)	0.378(2)	0.449(3)	C(301)*	0.359(6)	0.513(7)	0.780(3)
C(24)	0.877(2)	0.359(3)	0.529(2)	Cl(1)*	0.436(3)	0.526(2)	0.902(2)
C(25)	0.781(3)	0.282(3)	0.550(2)	Cl(2)*	0.191(3)	0.545(2)	0.786(2)
C(26)	0.633(3)	0.225(2)	0.491(2)				

* For the CH_2Cl_2 molecule of crystallisation.

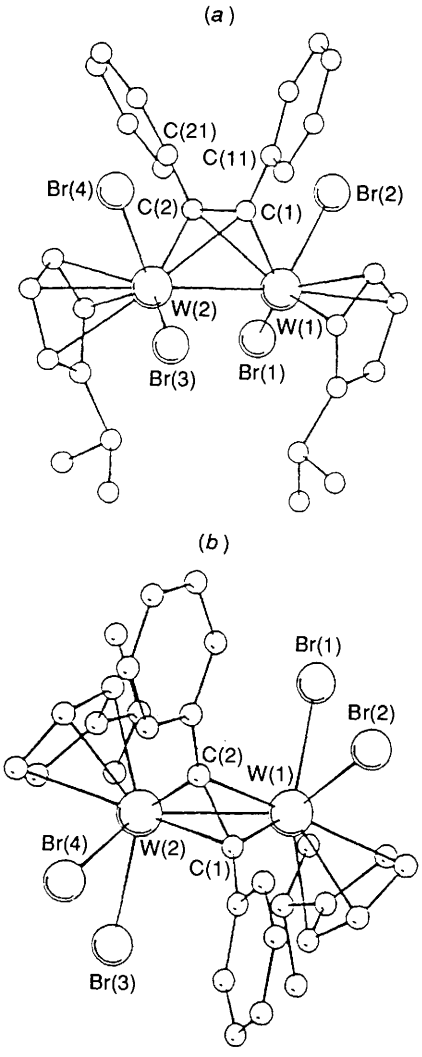

Fig. 1 Two views of the molecular structure of $[W_2(\eta\text{-}C_5H_4Pr^i)_2Br_4(\mu\text{-}C_2Ph_2)]$ **7**: (*a*) nearly perpendicular to the W–W bond, (*b*) along the molecular C_2 axis. Hydrogen atoms omitted for clarity

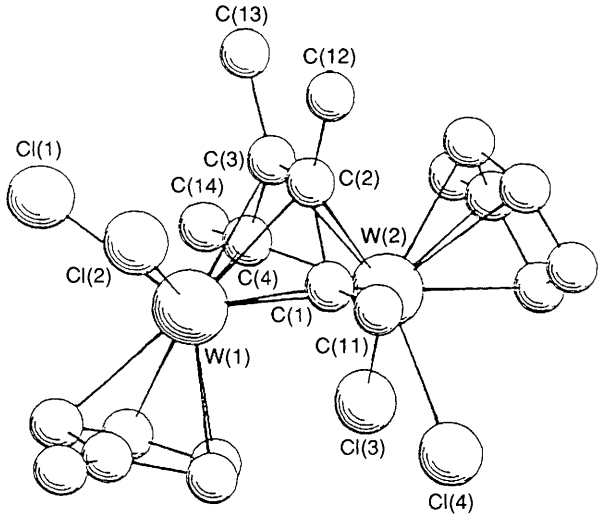

Fig. 2 Molecular structure of *trans*-$[W_2(\eta\text{-}C_5H_4Me)_2Cl_4(\mu\text{-}C_4Me_4)]$ **12b**. Hydrogen atoms omitted for clarity

respectively). The NMR spectra (Table 1) were very similar to those of **10a**. The compounds **10a**, **10b** and **11** isomerise in solution at room temperature over several days to give orange compounds **12a**, **12b** and **13** respectively of identical empirical formulae to those of their precursors. The NMR spectra of the orange compounds were largely similar to those of their purple precursors but now revealed two spectroscopically inequivalent $\eta\text{-}C_5H_4R$ rings. For **12a** and **13**, ^{183}W satellites [$^1J(C\text{–}^{183}W)$ 49 Hz, 25% of total signal intensity; ^{183}W, $I = \frac{1}{2}$, natural abundance = 14.5%] of the correct intensity for a carbon bonded to two tungsten atoms could be observed for the lowest-field quaternary carbon resonances. Single crystals of **12b** were obtained by slow diffusion of diethyl ether into a thf solution and an X-ray diffraction analysis was undertaken. The molecular structure is shown in Fig. 2, selected bond lengths and angles are given in Table 4 and fractional atomic coordinates in Table 5.

Table 4 Selected bond lengths (Å) and angles (°) with e.s.d.s in parentheses for $[W_2(\eta\text{-}C_5H_4Me)_2Cl_4(\mu\text{-}C_4Me_4)]$ **12b**; $Cp_{cent(1)}$ and $Cp_{cent(2)}$ refer to the computed $\eta\text{-}C_5H_4Me$ ring centroids for W(1) and W(2) respectively

W(1)–Cl(1)	2.486(3)	W(2)–Cl(3)	2.481(1)
W(1)–Cl(2)	2.474(4)	W(2)–Cl(4)	2.471(4)
W(1)–C(1)	2.11(1)	W(2)–C(1)	2.11(1)
W(1)–C(2)	2.39(1)	W(2)–C(2)	2.38(2)
W(1)–C(3)	2.36(2)	W(2)–C(3)	2.38(1)
W(1)–C(4)	2.10(2)	W(2)–C(4)	2.10(1)
W(1)–$Cp_{cent(1)}$	1.99	W(2)–$Cp_{cent(2)}$	2.06
C(1)–C(2)	1.46(2)	C(1)–C(11)	1.52(2)
C(2)–C(3)	1.44(2)	C(2)–C(12)	1.50(2)
C(3)–C(4)	1.43(2)	C(3)–C(13)	1.51(2)
C(4)–C(14)	1.53(2)	W(1)–W(2)	2.9295(7)
Cl(1)–W(1)–W(2)	125.7(1)	Cl(2)–W(1)–W(2)	125.4(1)
Cl(3)–W(2)–W(1)	98.8(8)	Cl(4)–W(2)–W(1)	96.8(1)
Cl(2)–W(1)–Cl(1)	77.7(2)	Cl(3)–W(2)–Cl(4)	78.6(1)
W(1)–C(1)–W(2)	88.0(5)	W(1)–C(2)–W(2)	75.6(4)
W(1)–C(3)–W(2)	76.3(4)	W(1)–C(4)–W(2)	88.4(6)
C(11)–C(1)–C(2)	121.3(13)	C(12)–C(2)–C(1)	121.9(15)
C(13)–C(3)–C(4)	122.2(16)	C(14)–C(4)–C(3)	121.9(16)
C(12)–C(2)–C(3)	119.4(15)	C(13)–C(3)–C(2)	117.2(13)
C(1)–C(2)–C(3)	118.6(13)	C(2)–C(3)–C(4)	120.6(15)

Angle between least-squares plane C(1)–C(4) and plane containing W(1) and W(2) is 89.8°.

Table 5 Fractional atomic coordinates ($\times 10^4$) for the non-hydrogen atoms of $[W_2(\eta\text{-}C_5H_4Me)_2Cl_4(\mu\text{-}C_4Me_4)]$ **12b**

Atom	*x*	*y*	*z*
W(1)	9 928.3(5)	937.7(4)	6 561.6(2)
W(2)	10 063.8(5)	2 547.0(4)	5 819.9(2)
Cl(1)	9 997(5)	1 052(3)	7 548(1)
Cl(2)	11 500(3)	−153(4)	6 787(2)
Cl(3)	8 028(3)	2 954(3)	5 774(2)
Cl(4)	9 475(3)	1 660(3)	5 017(1)
C(1)	11 009(11)	1 287(10)	5 922(5)
C(2)	11 553(13)	1 868(12)	6 332(6)
C(3)	10 853(12)	2 415(12)	6 687(6)
C(4)	9 650(11)	2 417(13)	6 628(6)
C(11)	1 697(13)	691(13)	5 535(6)
C(12)	12 808(11)	1 871(15)	6 408(8)
C(13)	11 441(16)	2 970(16)	7 123(7)
C(14)	8 886(16)	3 009(14)	6 991(6)
C(101)	9 065(13)	−630(11)	6 426(6)
C(102)	9 049(14)	−70(11)	5 957(6)
C(103)	8 365(11)	749(12)	6 062(7)
C(104)	8 026(10)	737(12)	6 598(7)
C(105)	8 482(13)	−109(13)	6 816(9)
C(106)	9 590(14)	−1 599(11)	6 467(7)
C(201)	10 232(12)	4 262(10)	5 771(5)
C(202)	11 295(12)	3 836(11)	5 876(7)
C(203)	11 664(15)	3 279(14)	5 438(7)
C(204)	10 840(15)	3 366(13)	5 033(7)
C(205)	9 956(16)	3 912(11)	5 258(5)
C(206)	599(21)	4 951(13)	6 100(9)

The solid-state structure of complex **12b** consists of two staggered, mutually *trans* $W(\eta\text{-}C_5H_4Me)Cl_2$ fragments linked by a metal–metal bond [W(1)–W(2) 2.9295(7) Å] which is bridged by a planar C_4Me_4 fragment. The $\mu\text{-}C_4Me_4$ moiety is symmetrically bound to each tungsten atom in a tetrahapto fashion and is perpendicular to the W–W bond. Its planarity and the trigonal geometry about each internal (quaternary) carbon atom (as indicated by each of the six Me–C–C angles being very close to 120°) suggests that each internal carbon atom is formally sp^2 hybridised. These observations, together with the equivalence of the three internal carbon–carbon bond lengths (within experimental error), indicate a high degree of delocalisation of the π electrons of this fragment. The X-ray and ^{13}C NMR data suggest a description intermediate between a buta-1,3-dienyl(2−) and but-2-enyl(4−) representation for the $\mu\text{-}C_4Me_4$ moiety. The similarity of the NMR data of **12a** and **13** to those of **12b** suggests that the former have similar formulations, *i.e.* $[W_2(\eta\text{-}C_5H_4Pr^i)_2X_4(\mu\text{-}C_4Me_4)]$ (X = Cl **12a** or Br **13**).

The ^{13}C NMR chemical shifts for the terminal quaternary carbon atoms of the $\mu\text{-}C_4Me_4$ fragment in complexes **12a** and **13** (δ 185.4 and 181.8 respectively) are suggestive of some degree of alkylidene character. In general, such shifts for authentic bridging alkylidene carbon atoms [M(μ-*C*RR′)M] fall in the range δ 100–210.[12] In the flyover bridge complex $[Cr_2(\eta\text{-}C_5H_5)_2(CO)(\mu\text{-}C_4Ph_4)]$ the terminal carbon atoms of the $\mu\text{-}C_4Ph_4$ fragment are equidistant from each Cr atom and their ^{13}C chemical shift (δ 210) suggests that these too have substantial alkylidene character.[13]

Given the similarity of their NMR spectra to those of **12a**, **12b** and **13**, we propose that the purple compounds **10a**, **10b** and **11** are the corresponding isomers *cis*-$[W_2(\eta\text{-}C_5H_4R)_2X_4(\mu\text{-}C_4Me_4)]$ (X = Cl, R = Pr^i **10a** or Me **10b**; X = Br, R = Pr^i **11**). However, the spectroscopic data alone do not allow one to distinguish between the two possible isomers possessing the C_{2v} symmetry required by the NMR spectra in which the $\eta\text{-}C_5H_4R$ rings are either *cis* or *trans* to the flyover bridge moiety (see Scheme 1).

The compounds **10–13** are uncommon examples of binuclear flyover bridge compounds in which the $\mu\text{-}C_4R_4$ fragment bonds symmetrically in a tetrahapto fashion to both metal atoms, the only other example being $[Mo_2(\eta\text{-}C_5H_5)_2Cl_2(\mu\text{-}C_4Ph_4)]$.[14] By far the most common form of co-ordination found for a flyover bridge arrangement is as $[L_nM\{\mu\text{-}(\sigma^2:\eta^4)\text{-}C_4R_4\}ML_m]$ which may be described as containing a metallacyclopentadiene ($L_nMC_4R_4$) fragment bound in pentahapto fashion to a second metal centre.[1,2] Cotton and Shang[15] have recently described a tetranuclear niobium complex in which two Nb–Nb bonds are bridged by symmetrically ($\mu\text{-}\eta^4:\eta^4$) bound C_4Ph_4 units.

We note that the *cis* ⟶ *trans* isomerisation of $[W_2(\eta\text{-}C_5H_4R)_2Cl_4(\mu\text{-}C_4Me_4)]$ also occurs quantitatively in the solid state at *ca.* 250 °C and is a very rare example of the solid-state isomerisation of an organometallic species.

Treatment of a toluene solution of pure $[W_2(\eta\text{-}C_5H_4Pr^i)_2Cl_4(\mu\text{-}C_2Et_2)]$ **3** with an excess of C_2Me_2 gave orange microcrystals of *trans*-$[W_2(\eta\text{-}C_5H_4Pr^i)_2Cl_4\{\mu\text{-}(1,2)\text{-}C_4Et_2Me_2\}]$ **14*** which were characterised by elemental analysis and by ^1H and ^{13}C NMR spectroscopy. Thus the ^1H NMR spectrum showed resonances typical of two diastereotopic $\eta\text{-}C_5H_4Pr^i$ rings together with two additional singlets at δ 2.16 and 3.45 assignable to two inequivalent methyl groups. There are also resonances arising from two independent ethyl groups, the methylene linkage for one of them appearing as a pair of mutually coupled doublets of quartets. The ^{13}C NMR spectra similarly revealed resonances assignable to two diastereotopic $\eta\text{-}C_5H_4Pr^i$ groups and to two inequivalent methyl and ethyl groups. Four further singlet carbon resonances were observed at δ 193.7 and 185.5 (assigned as the 1- and 4-quaternary carbon atoms of a $\mu\text{-}C_4R_2R'_2$ fragment) and at δ 93.9 and 89.8 (assigned as the 2- and 3-quaternary carbon atoms of a $\mu\text{-}C_4R_2R'_2$ fragment). On the basis of these data the structure illustrated in Scheme 1 is proposed for **14** in which a C_2Me_2 fragment has inserted into one of the W–C_{ac} bonds of **3**; this is consistent with the mechanisms postulated for other coupled alkyne systems.[1,2]

When the reaction between complex **3** and C_2Me_2 was monitored by ^1H NMR spectroscopy, resonances assignable to the *cis* isomer of **14** were observed, but this compound was not isolated. Moreover, no resonances were observed for compounds containing a $\mu\text{-}C_4Me_4$ unit (*i.e.* compounds **10a** or **12a**), suggesting that if alkyne exchange of the monoalkyne adduct **3** occurs at all then it is at a very slow rate compared to that of the alkyne coupling reaction. Products containing a $\mu\text{-}(1,3)\text{-}C_4Et_2Me_2$ or $\mu\text{-}(1,4)\text{-}C_4Et_2Me_2$ linkage were not observed but may be prepared from the reaction of **1a** with pent-2-yne.

Thus treatment of a toluene solution of complex **1a** with an excess of EtC_2Me at room temperature gave a small quantity of a purple solid **15** and an orange supernatant. Compound **15** was identified as *cis*-$[W_2(\eta\text{-}C_5H_4Pr^i)_2Cl_4\{\mu\text{-}(1,4)\text{-}C_4Et_2Me_2\}]$ by elemental analysis and ^1H NMR spectroscopy. The ^1H NMR spectrum showed resonances assignable to two equivalent $\eta\text{-}C_5H_4Pr^i$ rings, a further two equivalent methyl groups at δ 1.80 and to two equivalent ethyl groups, the overall appearance of the spectrum showing that **15** has C_{2v} symmetry. Briefly heating solid **15** *in vacuo* at *ca.* 250 °C effected a colour change from purple to orange. The ^1H NMR spectrum of the product **16** now showed resonances characteristic of two $\eta\text{-}C_5H_4Pr^i$ ligand environments, and the protons of methylene linkages of the two equivalent ethyl groups appeared as a pair of mutually coupled doublets of quartets, the overall symmetry of the molecule now being C_s. On the basis of these data and a satisfactory elemental analysis, the compound is proposed to be the *trans* isomer of **15**, *trans*-$[W_2(\eta\text{-}C_5H_4Pr^i)_2Cl_4\{\mu\text{-}(1,4)\text{-}C_4Et_2Me_2\}]$ **16**.

Concentration of the orange supernatant from the above reaction under reduced pressure and cooling to −25 °C gave an orange microcrystalline material identified by ^1H NMR spectroscopy as a mixture of **16** and *trans*-$[W_2(\eta\text{-}C_5H_4Pr^i)_2Cl_4\{\mu\text{-}(1,3)\text{-}C_4Et_2Me_2\}]$ **17** in approximately 1:2 ratio. It was not possible to separate the μ-(1,3) and μ-(1,4) isomers, but signals due to **17** could be unambiguously assigned since the ^1H NMR spectrum of pure **16** was known. The ^1H NMR spectrum of **17** shows resonances assignable to two types of diastereotopic $\eta\text{-}C_5H_5Pr^i$ ligands, two different methyl groups, and to two different ethyl groups, the methylene protons of which appeared as doublets of quartets.

Monitoring the reaction of complex **1a** with pent-2-yne by ^1H NMR spectroscopy showed no evidence for the corresponding μ-(2,3)- or μ-(1,2) (*i.e.* compound **14**) isomers. In none of the alkyne coupling reactions could a third alkyne molecule be introduced into the μ-hydrocarbyl bridge.

In contrast to the reactions of $[W_2(\eta\text{-}C_5H_4Pr^i)_2Cl_4(\mu\text{-}C_2Et_2)]$ **3** described above, treatment of toluene solutions of the bromide-supported analogues $[W_2(\eta\text{-}C_5H_4Pr^i)_2Br_4(\mu\text{-}C_2R_2)]$ (R = Me **5** or Et **6**) with an excess of but-2-yne surprisingly gave no reaction even after prolonged heating. However, it was found that the poorly defined fluxional complexes $[\{W(\eta\text{-}C_5H_4Pr^i)Br_2(CR)\}_{3x}]$ (R = Me **8** or Et **9**) *do* react readily with added but-2-yne to give the flyover bridge complexes *cis*- and *trans*-$[W_2(\eta\text{-}C_5H_4Pr^i)_2Br_4(\mu\text{-}C_4Me_4)]$ (see above) or *cis*-$[W_2(\eta\text{-}C_5H_4Pr^i)_2Br_4\{\mu\text{-}(1,2)\text{-}C_4Et_2Me_2\}]$ **18** in *ca.* 80% yield. The latter complex isomerised slowly in dichloromethane solution over 2 h at room temperature (r.t.) to give the corresponding isomer *trans*-$[W_2(\eta\text{-}C_5H_4Pr^i)_2Br_4\{\mu\text{-}(1,2)\text{-}C_4Et_2Me_2\}]$ **19** in quantitative yield. The compounds **18** and **19** were characterised by elemental analysis and by ^1H and ^{13}C NMR spectroscopy (see Table 1). No evidence was found for formation of compounds containing μ-(1,3)-, μ-(2,3)- or $\mu\text{-}(1,4)\text{-}C_4Et_2Me_2$ linkages.

* The (*x*,*y*) notation refers to the positions of the Et groups in the $\mu\text{-}C_4Et_2Me_2$ fragment.

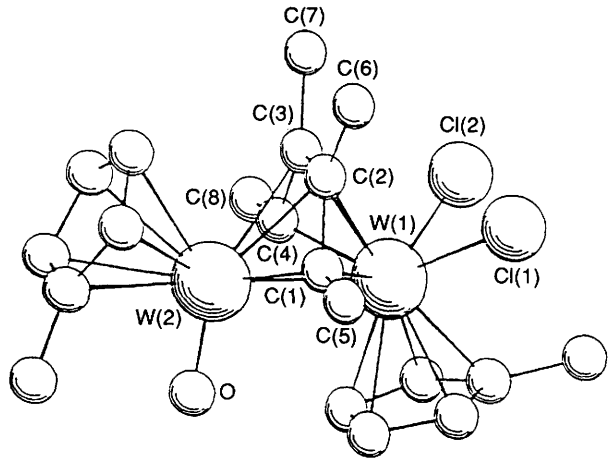

Fig. 3 Molecular structure of $[W_2(\eta\text{-}C_5H_4Me)_2Cl_2O(\mu\text{-}C_4Me_4)]$ **20b**. Hydrogen atoms omitted for clarity

Table 6 First-order rate constants (k_1) and half-lives ($t_{\frac{1}{2}}$) for the *cis* to *trans* isomerisation of related flyover-bridge complexes in [$^2H_6$]acetone at 336 K

Complex	$10^4k_1/s^{-1}$	$t_{\frac{1}{2}}$/min
$[W_2(\eta\text{-}C_5H_4Pr^i)_2Br_4(\mu\text{-}C_4Me_4)]$ [a]	1.67	71.0
$[W_2(\eta\text{-}C_5H_4Pr^i)_2Cl_4(\mu\text{-}C_4Me_4)]$ [b]	2.70	42.2
$[W_2(\eta\text{-}C_5H_4Pr^i)_2Br_4\{\mu\text{-}(1,2)\text{-}C_4Et_2Me_2\}]$ [c]	9.90	11.7

[a] *i.e.* for **11** ⟶ **13**. [b] *i.e* for **10a** ⟶ **12a**. [c] *i.e.* for **18** ⟶ **19**.

Table 7 Selected bond lengths (Å) and angles (°) with e.s.d.s in parentheses for $[W_2(\eta\text{-}C_5H_4Me)_2Cl_2O(\mu\text{-}C_4Me_4)]$ **20b**, $Cp_{cent(1)}$ and $Cp_{cent(2)}$ refer to the computed $\eta\text{-}C_5H_4Me$ ring centroids for W(1) and W(2) respectively

W(1)–Cl(1)	2.472(3)	W(1)–Cl(2)	2.475(3)
W(1)–W(2)	2.9097(6)	W(2)–O	1.71(1)
W(1)–C(1)	2.14(1)	W(2)–C(1)	2.10(1)
W(1)–C(2)	2.35(1)	W(2)–C(2)	2.49(1)
W(1)–C(3)	2.36(1)	W(2)–C(3)	2.49(1)
W(1)–C(4)	2.16(1)	W(2)–C(4)	2.09(1)
W(1)–$Cp_{cent(1)}$	1.99	W(2)–$Cp_{cent(2)}$	2.10
C(1)–C(2)	1.46(1)	C(1)–C(5)	1.51(1)
C(2)–C(3)	1.45(1)	C(2)–C(6)	1.52(1)
C(3)–C(4)	1.44(1)	C(3)–C(7)	1.52(1)
C(4)–C(8)	1.50(1)		
Cl(1)–W(1)–W(2)	127.51(8)	Cl(2)–W(1)–W(2)	127.18(8)
Cl(2)–W(1)–Cl(1)	79.3(1)	O–W(2)–W(1)	97.5(3)
W(2)–C(1)–W(1)	86.6(4)	W(2)–C(2)–W(1)	74.0(3)
W(2)–C(3)–W(1)	73.7(3)	W(2)–C(4)–W(1)	86.4(4)
C(5)–C(1)–C(2)	123.6(11)	C(6)–C(2)–C(1)	119.4(10)
C(7)–C(3)–C(4)	120.9(11)	C(8)–C(4)–C(3)	122.8(11)
C(6)–C(2)–C(3)	120.3(10)	C(7)–C(3)–C(2)	119.6(10)
C(1)–C(2)–C(3)	120.3(9)	C(2)–C(3)–C(4)	119.6(9)

Angle between least-squares plane C(1)–C(4) and plane containing W(1) and W(2) is 83.3°.

Further Studies of the cis ⟶ trans *Isomerisation Reactions.*—The activation energy (E_a) for the isomerisation of *cis*-$[W_2(\eta\text{-}C_5H_4Pr^i)_2Cl_4(\mu\text{-}C_4Me_4)]$ **10a** to *trans*-$[W_2(\eta\text{-}C_5H_4Pr^i)_2Cl_4(\mu\text{-}C_4Me_4)]$ **12a** has been determined by measuring the first-order rate constants (k_1) for this process at four temperatures using ^1H NMR spectroscopy. The rate constants were then fitted to the Arrhenius equation to yield E_a = 23.6(2) kcal mol^{-1} [98.8(8) kJ mol^{-1}]. The magnitude of E_a is consistent with the mechanism of the isomerisation process involving a 'simple' rotation of one $W(\eta\text{-}C_5H_4Pr^i)Cl_2$ fragment and effectively eliminates high-energy processes involving bond scission.

Table 8 Fractional atomic coordinates ($\times 10^4$) for the non-hydrogen atoms of $[W_2(\eta\text{-}C_5H_4Me)_2Cl_2O(\mu\text{-}C_4Me_4)]$ **20b**

Atom	*x*	*y*	*z*
W(1)	7 475.7(5)	1 251.2(2)	758.6(5)
W(2)	9 813.6(5)	1 021.5(2)	3 091.5(5)
Cl(1)	7 643(4)	1 835(1)	−1 462(3)
Cl(2)	5 273(4)	1 845(1)	939(4)
O	9 747(12)	325(4)	2 981(12)
C(1)	9 852(14)	1 339(5)	929(11)
C(2)	9 393(13)	1 858(4)	1 548(11)
C(3)	8 314(12)	1 869(4)	2 660(13)
C(4)	7 693(13)	1 365(5)	3 144(12)
C(5)	11 010(18)	1 291(7)	−184(18)
C(6)	10 028(18)	2 387(6)	990(16)
C(7)	7 834(18)	2 413(6)	3 276(17)
C(8)	6 570(15)	1 342(6)	4 285(15)
C(9)	5 915(12)	756(5)	−816(14)
C(10)	7 351(14)	585(6)	−1 093(14)
C(11)	7 918(16)	336(6)	241(17)
C(12)	6 888(16)	344(5)	1 310(15)
C(13)	5 607(15)	590(5)	604(14)
C(14)	4 765(15)	997(7)	−1 980(16)
C(15)	12 112(14)	850(5)	4 576(13)
C(16)	12 264(15)	1 337(5)	3 782(15)
C(17)	11 334(15)	1 723(6)	4 402(15)
C(18)	10 512(15)	1 454(5)	5 458(14)
C(19)	11 059(15)	916(5)	5 580(14)
C(20)	12 986(24)	325(8)	4 325(23)

We have also compared the rates of *cis* ⟶ *trans* isomerisation (from ^1H NMR spectroscopy in [$^2H_6$]acetone at 336 K) for the processes **10a** ⟶ **12a**, **11** ⟶ **13** and **18** ⟶ **19** and values obtained for k_1 are listed in Table 6 along with the associated half-lives ($t_{\frac{1}{2}}$). Comparison of the k_1 (or $t_{\frac{1}{2}}$) values in Table 6 shows that the isomerisation of the complexes *cis*-$[W_2(\eta\text{-}C_5H_4Pr^i)_2X_4\{\mu\text{-}(1,2)\text{-}C_4R_2Me_2\}]$ (X = Cl, R = Me **10a**; X = Br, R = Me **11** or Et **18**) is faster when R is bulkier, but slower when X is bulkier.

Hydrolysis Reactions of cis- *or* trans-$[W_2(\eta\text{-}C_5H_4R)_2Cl_4(\mu\text{-}C_4Me_4)]$ **10** *or* **12**.—Acetone solutions of *cis*- or *trans*-$[W_2(\eta\text{-}C_5H_4Pr^i)_2Cl_4(\mu\text{-}C_4Me_4)]$ **10a** or **12a** are moderately stable in air for several hours. However, addition of a small amount of water led to an immediate reaction and the cherry-red oxo compound $[W_2(\eta\text{-}C_5H_4Pr^i)_2Cl_2O(\mu\text{-}C_4Me_4)]$ **20a** was isolated in near-quantitative yield (see Scheme 1).

Compound **20a** was characterised by elemental analysis, IR and ^1H and ^{13}C NMR spectroscopy, and also by fast atom bombardment (FAB) mass spectrometry. The ^1H and ^{13}C NMR spectra were largely similar to those of *trans*-$[W_2(\eta\text{-}C_5H_4Pr^i)_2Cl_4(\mu\text{-}C_4Me_4)]$, showing resonances assignable to two inequivalent $\eta\text{-}C_5H_5Pr^i$ rings and to a $\mu\text{-}C_4Me_4$ fragment. Notably the ^{13}C chemical shift of the terminal quaternary carbon atoms of the $\mu\text{-}C_4Me_4$ fragment are shifted to substantially higher field (δ 158.1 compared to 188.3, 185.4, 185.7 and 181.8 for the tetrachloro complexes **10a**, **12a**, **11** and **13** respectively). This may suggest a lesser degree of alkylidene character (although the different inductive effects of O *vs.* Cl_2 should also be considered). Moreover, $^1J(C\text{–}^{183}W)$ for the terminal 1- and 4-) quaternary carbon atoms of the $\mu\text{-}C_4Me_4$ moiety in **20a** is 114 Hz (14% of total signal intensity), consistent with bonding predominantly to only one W atom. For the tetrachloro *trans* compounds **12a** and **13**, smaller $^1J(C\text{–}^{183}W)$ coupling constants (49 Hz) for the terminal $\mu\text{-}C_4Me_4$ quaternary carbon atoms were observed and the magnitude of the ^{183}W satellites (24% of total signal intensity) is consistent with equivalent bonding to both W atoms.

The FAB mass spectrum of complex **20a** showed a parent

envelope centred around m/z 776 as expected for $C_{24}H_{34}Cl_2OW_2$. The IR spectrum showed several bands in the region 950–800 cm^{-1}, but an unambiguous assignment of one of these as ν(W=O) was not possible. Single crystals of **20a** suitable for an X-ray structure analysis could not be obtained. However, slow diffusion of pentane into a toluene solution of the methylcyclopentadienyl homologue $[W_2(\eta\text{-}C_5H_4Me)_2Cl_2O(\mu\text{-}C_4Me_4)]$ **20b**, prepared from **10b** or **12b**, afforded dark red crystals and an X-ray structure determination was undertaken. The molecular structure is shown in Fig. 3, selected bond lengths and angles in Table 7, and fractional atomic coordinates in Table 8.

The overall molecular structure of complex **20b** is similar to that of **12b** (Fig. 2) and possesses a *trans* disposition of the η-C_5H_4Me rings with a terminal tungsten–oxygen double bond [W(2)–O(1) 1.71(1) Å] *trans* to a planar, bridging μ-C_4Me_4 moiety. The W=O bond length in **20b** is similar to that found for other oxo tungsten systems.[16] A particularly interesting feature is that the μ-C_4Me_4 fragment is no longer symmetrically bound to each W atom. The terminal quaternary carbon atoms [C(1) and C(4)] bond more tightly to W(2) whereas the internal quaternary carbon atoms [C(2) and C(3)] bond more tightly to W(1). These observations are consistent with the ^{13}C NMR data described above for the more soluble isopropylcyclopentadienyl homologue, **20a**. The overall deviation (φ) of the μ-C_4Me_4 fragment from perpendicular (*i.e.* to the W–W bond) is *ca.* 7°.

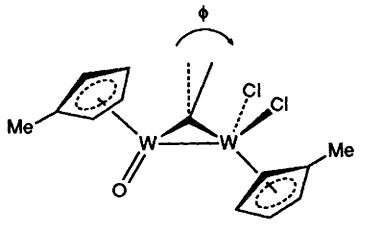

The asymmetry of the μ-C_4Me_4 fragment binding may reflect competition between the terminal oxo and μ-C_4Me_4 fragment π-electron systems for vacant orbitals on the metal atom. Other structural evidence for the strong *trans* influence of a terminal oxo ligand on a η-hydrocarbyl moiety has recently been reported: the formally pentahapto pentamethylcyclopentadienyl ring in $[W(\eta\text{-}C_5Me_5)O_2(OC_5Me_5)]$ exhibits a significant amount of σ,η^4 character.[17] The compounds **20a** and **20b** are the first examples of hydrocarbyl-bridged oxoditungsten species. The μ_3-alkyne trinuclear cluster $[W(\eta\text{-}C_5H_5)O][W(\eta\text{-}C_5H_5)(CO)_2][Fe(CO)_3]\{\mu\text{-}C_2(4\text{-}C_6H_4Me)_2\}$ has been described previously.[18]

Experimental

All manipulations of air- and moisture-sensitive materials were performed using either standard Schlenk-line techniques under an atmosphere of dinitrogen, which had been purified by passage over BASF catalyst and 4 Å molecular sieves, or in an inert-atmosphere dry-box containing dinitrogen unless stated otherwise. Solvents (unless stated otherwise) were predried by standing over 4 Å molecular sieves and then distilled under an atmosphere of dinitrogen from phosphorus pentaoxide (dichloromethane), sodium (toluene), potassium–benzophenone (thf), or sodium–potassium alloy (1:3 w/w) [light petroleum (b.p. 40–60 °C throughout), diethyl ether, pentane]. Deuteriated solvents for NMR studies were stored in Young's ampoules under an atmosphere of dinitrogen over sodium–potassium alloy ([$^2H_6$]benzene), molecular sieves ([$^2H_2$]dichloromethane) or as received ([$^2H_6$]acetone).

Proton and ^{13}C NMR spectra were recorded on a Brüker AM 300 spectrometer (^1H 300 MHz, ^{13}C 75.5 MHz), referenced internally using the residual protio solvent (^1H) or solvent (^{13}C) resonances relative to tetramethylsilane (δ = 0). Infrared spectra were recorded as CsI disks using a Perkin-Elmer 1510 FT interferometer. Elemental analyses were performed by the analytical department of this laboratory. The compounds $[W_2(\eta\text{-}C_5H_4R)_2X_4]$ (X = Cl, R = Pr^i or Me; X = Br, R = Pr^i) were prepared as described previously.[3]

Preparations.—$[W_2(\eta\text{-}C_5H_4Pr^i)_2Cl_4(\mu\text{-}C_2Et_2)]$ **3**. A solution of $[W_2(\eta\text{-}C_5H_4Pr^i)_2Cl_4]$ (0.38 g, 0.53 mmol) in toluene (15 cm^3) was treated with hex-3-yne (0.8 g, 9.8 mmol) to give a finely divided grey-green precipitate. After 5 h the supernatant was decanted, the pale powder washed with toluene (10 cm^3) and light petroleum (2 × 10 cm^3) and dried *in vacuo*. Yield: 300 mg, 70%.

$[W_2(\eta\text{-}C_5H_4Pr^i)_2Cl_4\{\mu\text{-}C_2(SiMe_3)_2\}]$ **4**. A solution of $[W_2(\eta\text{-}C_5H_4Pr^i)_2Cl_4]$ (0.37 g, 0.51 mmol) in toluene (20 cm^3) was treated with bis(trimethylsilyl)ethyne (0.1 g, 0.59 mmol) in thf (5 cm^3) to give a brown solution after 4 h. The volatiles were removed under reduced pressure and the residues washed thoroughly with light petroleum (4 × 15 cm^3). Extraction of the residues with diethyl ether (3 × 10 cm^3), reduction in volume to *ca.* 10 cm^3 and subsequent cooling to −80 °C afforded brown microcrystals of complex **4**. Yield: 180 mg (40%).

$[W_2(\eta\text{-}C_5H_4Pr^i)_2Br_4(\mu\text{-}C_2Me_2)]$ **5**. A solution of $[W_2(\eta\text{-}C_5H_4Pr^i)_2Br_4]$ (0.2 g, 0.22 mmol) in toluene (20 cm^3) was treated with 1 equivalent of but-2-yne (12 mg, 0.22 mmol) to give an orange-red solution after 1 d at r.t. Subsequent filtration, concentration to *ca.* 10 cm^3 and addition of light petroleum gave orange-red microcrystals of complex **5** on cooling to −20 °C. Yield: 130 mg (60%).

$[W_2(\eta\text{-}C_5H_4Pr^i)_2Br_4(\mu\text{-}C_2Et_2)]$ **6**. A solution of $[W_2(\eta\text{-}C_5H_4Pr^i)_2Br_4]$ (0.2 g, 0.22 mmol) in toluene (20 cm^3) was treated with 1 equivalent of hex-3-yne (18 mg, 0.22 mmol) to give an orange-red solution after 2 d at r.t. Subsequent filtration, concentration to *ca.* 10 cm^3 and addition of light petroleum gave orange-red microcrystals of complex **6** on cooling to −80 °C. Yield: 120 mg (60%).

$[W_2(\eta\text{-}C_5H_4Pr^i)_2Br_4(\mu\text{-}C_2Ph_2)]$ **7**. A solution of $[W_2(\eta\text{-}C_5H_4Pr^i)_2Br_4]$ (0.2 g, 0.22 mmol) in toluene (20 cm^3) was treated with 1 equivalent of diphenylethyne (40 mg, 0.22 mmol) to give an orange-red precipitate after 12 h at r.t. The supernatant was decanted and the precipitate was washed with light petroleum (2 × 10 cm^3) and dried *in vacuo*. Recrystallisation from dichloromethane–light petroleum afforded orange-red microcrystals of **7**. Yield: 160 mg (70%).

$[\{W(\eta\text{-}C_5H_4Pr^i)Br_2(CMe)\}_{3x}]$ **8**. A suspension of $[W_2(\eta\text{-}C_5H_4Pr^i)_2Br_4]$ (0.2 g, 0.22 mmol) in diethyl ether (20 cm^3) was treated with an excess of but-2-yne (0.2 g, 3.7 mmol) to give a brown-green precipitate after stirring for 1 h at −20 °C. The pale supernatant was decanted and the precipitate was washed with light petroleum (2 × 10 cm^3) and dried *in vacuo* to give compound **8**. Yield: 180 mg.

$[\{W(\eta\text{-}C_5H_4Pr^i)Br_2(CEt)\}_{3x}]$ **9**. A suspension of $[W_2(\eta\text{-}C_5H_4Pr^i)_2Br_4]$ (0.2 g, 0.22 mmol) in diethyl ether (20 cm^3) was treated with an excess of hex-3-yne (0.1 g, 1.2 mmol) to give a grey-green precipitate after 1 h at r.t. The pale supernatant was decanted and the precipitate was washed with light petroleum (2 × 10 cm^3) and dried *in vacuo* to give compound **9**. Yield: 190 mg.

cis-$[W_2(\eta\text{-}C_5H_4R)_2Cl_4(\mu\text{-}C_4Me_4)]$ (R = Pr^i **10a** *or* Me **10b**). A solution of $[W_2(\eta\text{-}C_5H_4R)_2Cl_4]$ (0.3 mmol) in toluene (30 cm^3) was treated with an excess of but-2-yne and allowed to stand for 20 h. The red-brown supernatant was decanted and the purple solid washed with toluene (10 cm^3) and light petroleum (2 × 10 cm^3) and dried *in vacuo* to give analytically pure complex **10a** or **10b**. Yield: *ca.* 60%.

cis-$[W_2(\eta\text{-}C_5H_4Pr^i)_2Br_4(\mu\text{-}C_4Me_4)]$ **11**. A solution of $[W_2(\eta\text{-}C_5H_4Pr^i)_2Br_4]$ (0.2 g, 0.22 mmol) in diethyl ether (20 cm^3) was treated with an excess of but-2-yne (0.2 g, 3.7 mmol) to give a red-brown solution and purple precipitate after 30 min at r.t. The supernatant was decanted and the precipitate was washed with light petroleum (2 × 10 cm^3) and dried *in vacuo* to give analytically pure complex **11**. Yield: 148 mg (60%).

Table 9 Crystal data, data collection and processing parameters for $[W_2(\eta\text{-}C_5H_4Pr^i)_2Br_4(\mu\text{-}C_2Ph_2)]\cdot 0.5CH_2Cl_2$ **7**·$0.5CH_2Cl_2$, *trans*-$[W_2(\eta\text{-}C_5H_4Me)_2Cl_4(\mu\text{-}C_4Me_4)]$ **12b** and $[W_2(\eta\text{-}C_5H_4Me)_2Cl_2O(\mu\text{-}C_4Me_4)]$ **20b**

	7·$0.5CH_2Cl_2$	**12b**	**20b**
Formula	$C_{30}H_{32}Br_4W_2\cdot 0.5CH_2Cl_2$	$C_{20}H_{26}Cl_4W_2$	$C_{20}H_{26}Cl_2OW_2$
M	1122.37	775.94	721.03
Crystal size/mm	0.10 × 0.30 × 0.30	0.10 × 0.30 × 0.35	Irregular
Crystal system	Triclinic	Orthorhombic	Monoclinic
Space group	$P\bar{1}$	*Pbca*	$P2_1/n$
a/Å	9.569(8)	11.847(2)	9.006(3)
b/Å	14.326(8)	14.001(2)	24.271(5)
c/Å	14.803(6)	25.148(4)	9.005(3)
α/°	113.80(4)		
β/°	96.75(5)		94.51(3)
γ/°	106.09(6)		
U/Å^3	1722.1	4171.8	1978.3
Z	2	8	4
D_c/g cm^{-3}	2.18	2.47	2.42
μ/cm^{-1}	115.2	117.8	121.6
F(000)	1054	2896	1344
2θ limits/°	2–36	3–50	3–50
ω scan width (+0.35 tanθ)/°	0.75	0.50	0.55
Total data collected	2831	4945	4407
Total unique data	2363	3650	3469
No. of observations [$I > 3\sigma(I)$]	1409	2118	3106
R(merge)	0.073	0.047	0.042
No. of variables	120	236	216
Obs./variables	11.7	8.97	14.37
Weighting coefficients	6.14, 0.437, 3.32	Unit weights	9.22, −0.13, 5.79, 2.91
Maximum, minimum peak in final difference map/e Å^3	3.4, −0.3	0.9, −0.1	1.2, −0.2
R^a	0.077	0.029	0.068
R'^b	0.091	0.031	0.071

^{a} $R = \Sigma||F_o| - |F_c||/\Sigma|F_o|$. ^{b} $R' = [\Sigma w(|F_o| - |F_c|)^2/\Sigma w|F_o|^2]^{\frac{1}{2}}$.

trans-$[W_2(\eta\text{-}C_5H_4R)_2Cl_4(\mu\text{-}C_4Me_4)]$ (R = Pr^i **12a** *or* Me **12b**). *Method* (*i*). A solution of *cis*-$[W_2(\eta\text{-}C_5H_4R)_2Cl_4(\mu\text{-}C_4Me_4)]$ (R = Pr^i **10a** or Me **10b** in thf was allowed to stand for 96 h at r.t. to give an orange solution. The volatiles were removed under reduced pressure and the residues extracted with toluene. Subsequent reduction in volume and cooling to −80 °C afforded orange microcrystals of complex **12a** or **12b**. Yield: *ca.* 80%.

Method (*ii*). Solid *cis*-$[W_2(\eta\text{-}C_5H_4R)_2Cl_4(\mu\text{-}C_4Me_4)]$ (R = Pr^i **10a** or Me **10b** was placed in a Schlenk tube and briefly heated under reduced pressure with a cool blue flame. The colour changed immediately from purple to orange affording analytically pure complex **12a** or **12b** in quantitative yield.

trans-$[W_2(\eta\text{-}C_5H_4Pr^i)_2Br_4(\mu\text{-}C_4Me_4)]$ **13**. A purple solution of *cis*-$[W_2(\eta\text{-}C_5H_4Pr^i)_2Br_4(\mu\text{-}C_4Me_4)]$ **11** in CH_2Cl_2 was allowed to stand for 12 h at r.t. to give an orange-red solution. The volatiles were removed under reduced pressure and the residues extracted with toluene (2 × 10 cm^3). Subsequent filtration, concentration to *ca.* 10 cm^3 and addition of light petroleum gave orange-red microcrystals of complex **11** on cooling to −80 °C. Yield: *ca.* 80%.

trans-$[W_2(\eta\text{-}C_5H_4Pr^i)_2Cl_4\{\mu\text{-}(1,2)\text{-}C_4Et_2Me_2\}]$ **14**. A solution of $[W_2(\eta\text{-}C_5H_4Pr^i)_2Cl_4(\mu\text{-}C_2Et_2)]$ **3** (0.22 g, 0.27 mmol) in thf (15 cm^3) was treated with an excess of but-2-yne (0.4 g, 7 mmol) to give a cherry-red solution. After 7 h the volatiles were removed under reduced pressure and the residues extracted with toluene (3 × 15 cm^3). Reduction in volume and cooling to −80 °C afforded orange microcrystals of complex **14** which were washed with cold toluene (5 cm^3) and light petroleum (2 × 10 cm^3) and dried *in vacuo*. Yield: 180 mg (77%).

cis-$[W_2(\eta\text{-}C_5H_4Pr^i)_2Cl_4\{\mu\text{-}(1,4)\text{-}C_4Et_2Me_2\}]$ **15**. A solution of $[W_2(\eta\text{-}C_5H_4Pr^i)_2Cl_4]$ (0.4 g, 0.55 mmol) in toluene (20 cm^3) was treated with pent-2-yne (0.7 g, 10 mmol) to give an orange-brown solution and a small quantity of purple solid after 30 h at r.t. The supernatant was decanted and the solid washed with toluene and light petroleum and dried *in vacuo* to give analytically pure complex **15**. Yield: 85 mg (20%).

trans-$[W_2(\eta\text{-}C_5H_4Pr^i)_2Cl_4\{\mu\text{-}(1,4)\text{-}C_4Et_2Me_2\}]$ **16**. Solid *cis*-$[W_2(\eta\text{-}C_5H_4Pr^i)_2Cl_4\{\mu\text{-}(1,4)\text{-}C_4Et_2Me_2\}]$ **15** was placed in a Schlenk tube and briefly heated under reduced pressure with a cool blue flame. The colour changed immediately from purple to orange affording analytically pure complex **16** in quantitative yield.

trans-$[W_2(\eta\text{-}C_5H_4Pr^i)_2Cl_4\{\mu\text{-}(1,3)\text{-}C_4Et_2Me_2\}]$ **17**. This compound was obtained as the major component of a *ca.* 1:2 mixture of **16** and **17**. Concentration of the orange-brown supernatant from the preparation of **15** (see above) and cooling to −80 °C afforded a *ca.* 1:2 (by ^{1}H NMR spectroscopy) mixture of **16** and **17** as orange microcrystals. These were washed with cold toluene (2 × 5 cm^3) and light petroleum (2 × 10 cm^3) and dried *in vacuo*. Yield: 230 mg.

cis-$[W_2(\eta\text{-}C_5H_4Pr^i)_2Br_4\{\mu\text{-}(1,2)\text{-}C_4Et_2Me_2\}]$ **18**. A solution of $[\{W(\eta\text{-}C_5H_4Pr^i)Br_2(CEt)\}_{3x}]$ **9** (0.2 g) in thf (20 cm^3) was treated with but-2-yne (0.2 g, 3.7 mmol) to give a red-purple solution after 12 h at r.t. Subsequent filtration, concentration to *ca.* 10 cm^3 and addition of light petroleum gave red-purple microcrystals of complex **18** on cooling to −80 °C. Yield: 168 mg (80%).

trans-$[W_2(\eta\text{-}C_5H_4Pr^i)_2Br_4\{\mu\text{-}(1,2)\text{-}C_4Et_2Me_2\}]$ **19**. A purple solution of *cis*-$[W_2(\eta\text{-}C_5H_4Pr^i)_2Br_4\{\mu\text{-}(1,2)\text{-}C_4Et_2Me_2\}]$ **18** in CH_2Cl_2 was allowed to stand for 1 d at r.t. to give an orange-red solution. The volatiles were removed under reduced pressure and the residues extracted with toluene (2 × 10 cm^3). Reduction in volume and cooling to −80 °C afforded orange-red microcrystals of complex **19**. Yield: *ca.* 80%.

$[W_2(\eta\text{-}C_5H_4R)_2Cl_2O(\mu\text{-}C_4Me_4)]$ (R = Pr^i **20a** *or* Me **20b**). A solution of *cis*- or *trans*-$[W_2(\eta\text{-}C_5H_4R)_2Cl_4(\mu\text{-}C_4Me_4)]$ (0.36 mmol) in acetone (15 cm^3, technical grade) was treated in air with water (2 cm^3) to give a cherry-red solution after 2 h. The volatiles were removed under reduced pressure and the residues

crystallised from toluene (**20a**) or dichloromethane–toluene (1:1 v/v, **20b**) to give the required compounds as dark red microcrystals. Yield: *ca.* 80%.

X-Ray Crystal Structure Determinations of Complexes **7**, **12b** *and* **20b**.—Crystal data and data collection and processing parameters are given in Table 9. The general procedure was as follows. A crystal was sealed in a Lindemann glass capillary and transferred to the goniometer head of an Enraf-Nonius CAD4 diffractometer interfaced to a PDP 11/23 minicomputer. Unit-cell parameters were calculated from the setting angles of 25 reflections. Three reflections were chosen as intensity standards and were measured every 3600 s of X-ray exposure time, and three orientation controls were measured every 250 reflections. The data were measured using graphite-monochromated Mo-Kα radiation (λ = 0.710 69 Å) and an ω–2θ scan mode. An apparent unit cell transformation for complex **20b** was investigated but found not to possess full orthorhombic symmetry.

The data were corrected for Lorentz and polarisation effects and an empirical absorption correction[19] based on azimuthal scan data was applied. Equivalent reflections were merged and systematically absent reflections rejected. The tungsten atom positions were determined from a Patterson synthesis. Subsequent Fourier difference syntheses revealed the positions of other non-hydrogen atoms. For complexes **12b** and **20b** non-hydrogen atoms were refined with anisotropic thermal parameters by full-matrix least-squares procedures. Data collection and structure refinement for **7** proved to be problematic. Isotropic crystal decay during data collection (as monitored by three intensity controls) was *ca.* 65% and data could only be collected to $2\theta_{max}$ = 36°. Only the heavy atoms (W and Br) could be successfully subjected to anisotropic refinement; the remainder of the molecule was refined using 'rigid body' approximations (applied to the C_6H_5, Pr^i and C_5H_4 fragments) and self-consistent 'soft restraints'[20] to preserve the molecular C_2 symmetry. A final Fourier difference synthesis revealed substantial residual electron density which was successfully modelled as a molecule of dichloromethane of one half occupancy per asymmetric unit. The final residuals (Table 9) are satisfactory given the difficulties described above. For all three molecules, hydrogen atoms were placed in estimated positions (C–H 0.96 Å) with fixed isotropic thermal parameters and refined riding their supporting carbon atoms.

For complexes **7** and **20b** a Chebyshev weighting scheme[21] was applied and for all the compounds the data were corrected for the effects of anomalous dispersion and isotropic extinction (*via* an overall isotropic extinction parameter[22]) in the final stages of refinement. All crystallographic calculations were performed using the CRYSTALS suite[23] on a Micro VAX 3800 computer in the Chemical Crystallography Laboratory, Oxford. Neutral atom scattering factors were taken from ref. 24.

Additional material available from the Cambridge Crystallographic Data Centre comprises H-atom coordinates, thermal parameters, and remaining bond lengths and angles.

Acknowledgements

We thank the Chinese Government for support (to Q. F.), the SERC and BP plc for a CASE award (to P. M.) and P. C. McGowan for assistance with measuring NMR spectra.

References

1 M. J. Winter, *Adv. Organomet. Chem.*, 1989, **29**, 101.
2 W. A. Buhro and M. H. Chisholm, *Adv. Organomet. Chem.*, 1987, **27**, 311.
3 M. L. H. Green, J. D. Hubert and P. Mountford, *J. Chem. Soc., Dalton Trans.*, 1990, 3793.
4 M. L. H. Green and P. Mountford, *Organometallics*, 1990, **9**, 886.
5 F. A. Cotton and X. Feng, *Inorg. Chem.*, 1990, **29**, 3187.
6 D. L. Thorn and R. Hoffmann, *Inorg. Chem.*, 1978, **17**, 126.
7 M. J. Calhorda and R. Hoffmann, *Organometallics*, 1986, **5**, 2181.
8 W. I. Bailey, M. H. Chisholm, F. A. Cotton and L. A. Rankel, *J. Am. Chem. Soc.*, 1978, **100**, 5764; D. S. Ginley, C. R. Bock, M. S. Wrighton, B. Fischer, D. T. Tipton and R. Bau, *J. Organomet. Chem.*, 1978, **157**, 41.
9 M. H. Chisholm, K. Folting, D. M. Hoffman and J. C. Huffman, *J. Am. Chem. Soc.*, 1984, **106**, 6974.
10 K. J. Ahmed, M. H. Chisholm, K. Folting and J. C. Huffman, *Organometallics*, 1986, **5**, 2171.
11 S. G. Bott, D. L. Clark, M. L. H. Green and P. Mountford, *J. Chem. Soc., Dalton Trans.*, 1991, 471.
12 W. A. Herrman, *Adv. Organomet. Chem.*, 1982, **20**, 160.
13 S. A. R. Knox, R. F. D. Stansfield, F. G. A. Stone, M. J. Winter and P. Woodward, *J. Chem. Soc., Chem. Commun.*, 1978, 221.
14 W. Hispo and M. D. Curtis, *J. Am. Chem. Soc.*, 1988, **110**, 5218.
15 F. A. Cotton and M. Shang, *J. Am. Chem. Soc.*, 1990, **112**, 1584.
16 F. Bottomley and L. Sutin, *Adv. Organomet. Chem.*, 1988, **28**, 339; W. A. Nugent and J. M. Mayer, *Metal–Ligand Multiple Bonds*, Wiley-Interscience, New York, 1988.
17 G. Parkin, R. E. March, W. P. Schaefer and J. E. Bercaw, *Inorg. Chem.*, 1988, **27**, 3262.
18 L. Busetto, J. C. Jeffrey, R. M. Mills, F. G. A. Stone, M. J. Went and P. Woodward, *J. Chem. Soc., Dalton Trans.*, 1983, 101.
19 A. C. T. North, D. C. Philips and F. S. Mathews, *Acta Crystallogr., Sect. A*, 1968, **24**, 351.
20 D. J. Watkin, *Crystallographic Computing 4: Techniques and New Techniques*, eds. N. W. Isaacs and M. R. Taylor, Oxford University Press, Oxford, 1988 and refs. therein.
21 J. S. Rollet, *Computing Methods in Crystallography*, Pergamon, Oxford, 1965.
22 A. C. Larson, *Acta Crystallogr., Sect. A*, 1967, **23**, 664.
23 D. J. Watkin, J. R. Carruthers and P. W. Betteridge, *CRYSTALS User Guide*, Chemical Crystallography Laboratory, University of Oxford, 1985.
24 *International Tables for X-Ray Crystallography*, Kynoch Press, Birmingham, 1974, vol. 4.

Received 7th February 1992; *Paper* 2/00675H